2008

Landslide Susceptibility Zonation GIS for the 2005 Kashmir Earthquake affected region

Benjamin Growley
The University of Montana

LANDSLIDE SUSCEPTIBILITY ZONATION GIS FOR THE 2005 KASHMIR EARTHQUAKE AFFECTED REGION

By

Benjamin Justin Growley

Bachelor of Arts, Capital University, Columbus Ohio, 2003

Thesis Paper

presented in partial fulfillment of the requirements
for the degree of

Master of Arts
in Geography

The University of Montana
Missoula, MT

Spring 2008

Approved by:

Dr. David A. Strobel, Dean
Graduate School

Dr. Ulrich Kamp, Chair
Department of Geography

Dr. Sarah Halvorson
Department of Geography

Dr. Rebecca Bendick
Department of GeoSciences

Growley, Benjamin, Master of Arts, Spring 2008 Geography

Abstract Title: Landslide Susceptibility Zonation GIS for the 2005 Kashmir Earthquake Affected Region

Chairperson: Dr. Ulrich Kamp

The October 8, 2005 Kashmir earthquake triggered several thousand landslides throughout the Himalaya of northern Pakistan and India. A spatial database, which included 2252 landslides, was developed and analyzed using ASTER satellite imagery and geographical information system (GIS) technology. A multi-criterion evaluation was applied to determine the significance of event-controlling parameters in triggering the landslides. The parameters included lithology, faults, slope gradient, slope aspect, elevation, land cover, rivers and roads. The results were broken down into four classes of landslide susceptibility. The results indicated that lithology had the strongest influence on landsliding, particularly when the rock is highly fractured, such as in the shale, slate, clastic sediments, and limestone and dolomite. Moreover, the proximity of the landslides to faults, rivers, and roads was also an important factor in helping to initiate failures. In addition, landslides occurred particularly in moderate elevations on south facing slopes. Shrub land, grassland, and also agricultural land were highly susceptible to failures, while forested slopes had few landslides. One-third of the study area was highly or very highly susceptible to future landsliding and requires immediate mitigation action. The rest of the region had a low or moderate susceptibility to landsliding and remains relatively stable. This study supports the view that earthquake-triggered landslides are concentrated in specific zones associated with event-controlling parameters. It also concludes that western Himalaya deforestation and road construction are susceptible to landsliding during and shortly after earthquakes.

ACKNOWLEDGMENTS

This thesis could not have been written without the guidance of Dr. Ulrich Kamp, who not only was my committee chair, but also a good friend throughout my graduate career and beyond. With his help along with the help and patience of other University of Montana faculty- Dr. Sarah Halvorson, Dr. Rebecca Bendick and Dr. Anna Klene- I was able to successfully navigate my way through all the pitfalls and trials in the production of my Masters Thesis and graduate career.

I would like to thank Jennifer Hamilton for putting up with me in the field, always sending me helpful articles.

I would like to thank Dr. Lewis Owen and Ghazanfar Khattak from the University of Cincinnati, for their advice and assistance in field research. I would also like to thank Dr. Jose Roa from the University of Maryland, for always fully answering the questions I had, and then seven pages worth of answers to questions I did not know I had yet.

This project would not have been possible without the generous support of the National Science Foundation {EAR-0602675}, awarded to Dr. Ulrich Kamp and Dr. Lewis Owen and The University of Montana.

I greatly appreciate everyone in the Department of Geography. There was always was a helpful hand when any questions or technical difficulties arose.

TABLE OF CONTENTS

ABSTRACT II
ACKNOLOWDGEMENTS III
TABLE OF CONTENTS IV
LIST OF FIGURES VI
LIST OF TABLES VII

I. INTRODUCTION 1

1. THE EARTHQUAKE 1
2. OBJECTIVES 3
3. HYPOTHESES 4

II. BACKGROUND 6

1. THE 2005 KASHMIR EARTHQUAKE 6
2. SUSCEPTIBILITY MAPPING 6
3. LANDSLIDE CLASSIFICATION 9

III. STUDY AREA 11

IV. METHODOLOGY 16

1. FIELD WORK 16
2. GEOGRAPHICAL INFORMATION SYSTEM 16
3. SUSCEPTIBILITY MAPPING 17

V. LANDSLIDE INVENTORY MAPS 19

VI. ATTRIBUTE MAPS 20

1. GEOLOGY (LITHOLOGY) 20
2. FAULTS 26
3. LAND COVER 29
4. ELEVATION 35
5. SLOPE 35
6. ASPECT 36
7. ROADS, RIVERS, AND TRIBUTARIES 41

VII. PRE- AND POST-EARTHQUAKE LANDSLIDING 47

1. GEOLOGY (LITHOLOGY) 47
2. FAULTS 48
3. LAND COVER 49
4. ELEVATION 50
5. SLOPE 51
6. ASPECT 52
7. RIVERS, TRIBUTARIES, AND ROADS 53

VIII. MULTI-CRITERIA EVALUATION (MCE) 57

IX. LANDSLIDE SUSCEPTIBILITY 61

1. SUSCEPTIBILITY SUCCESS RATE 61
2. SUSCEPTIBILITY CLASSES 63
3. SUSCEPTIBILITY MAPS 64
4. LANDSLIDE INVENTORIES VERSUS LANDSLIDE SUSCEPTIBILITY 68

X. POST-SNOWMELT LANDSLIDING; REPEAT PHOTOGRAPHY 73

XII. CONCLUSION 81

1. LIMITATIONS OF STUDY 83
2. FURTHER RESEARCH 84

REFERENCES 86

LIST OF FIGURES

FIGURE 1. EARTHQUAKE EPICENTER IN AZAD JAMMU-KASHMIR IN NORTHEASTERN PAKISTAN 2
FIGURE 2. FATALITIES VS. MAGNITUDE FOR WORLDWIDE EARTHQUAKES SINCE 3
FIGURE 3. ASTER SATELLITE IMAGE OF THE STUDY AREA IN NORTHEASTERN PAKISTAN WITH MAJOR URBAN CENTERS AND EARTHQUAKE EPICENTER. 13
FIGURE 4. OBLIQUE THREE-DIMENSIONAL VIEW OF STUDY AREA**.** 14
FIGURE 5. EARTHQUAKE-TRIGGERED LANDSLIDING ALONG ROAD 15
FIGURE 6. EARTHQUAKE-TRIGGERED LANDSLIDING ALONG ROAD 15
FIGURE 7. GEOLOGIC MAP OF THE STUDY AREA. 24
FIGURE 8. PROFILE OF COLLISION ZONE BETWEEN INDIAN AND EURASIAN PLATES WITH INDUS-KOHISTAN SEISMIC ZONE**.** 26
FIGURE 9. FAULT LINES WITHIN STUDY AREA. 28
FIGURE 10. LAND COVER DISTRIBUTION WITHIN STUDY AREA. 33
FIGURE 11. LAND COVER CLASSES WITHIN THE STUDY AREA. 34
FIGURE 12. BAR GRAPH INDICATING A PERCENTAGE BREAKDOWN OF ELEVATION WITHIN THE STUDY AREA AT 500 METER CONTOUR INTERVAL 35
FIGURE 13. BAR GRAPH INDICATING A PERCENTAGE BREAKDOWN OF SLOPE WITHIN THE STUDY AREA.. 34
FIGURE 14. ELEVATION INTERVALS WITHIN THE STUDY AREA. 38
FIGURE 15. SLOPE CLASSES WITHIN STUDY AREA. 39
FIGURE 16. SLOPE ASPECT CLASSES WITHIN STUDY AREA. 40
FIGURE 17. EFFECTS OF ROAD AND RIVER CUTS ON HILL SLOPE STABILITY 47
FIGURE 18. LANDSLIDING ALONG A ROAD THAT WAS CUT INTO A STEEP SLOPE. 43
FIGURE 19. RIVERS FOUND WITHIN THE STUDY AREA. 44
FIGURE 20. TRIBUTARIES FOUND WITHIN THE STUDY AREA 45
FIGURE 21. ROADS FOUND WITHIN THE STUDY AREA. 46
FIGURE 22A. LANDSLIDE SUSCEPTIBILITY CURVE 2001 62
FIGURE 22B. LANDSLIDE SUSCEPTIBILITY CURVE 2001 62
FIGURE 23. FINAL SUSCEPTIBILITY MAP FOR 2001 65
FIGURE 24. FINAL SUSCEPTIBILITY MAP FOR 2005 63
FIGURE 25. MAP SHOWING THE 2005 LANDSLIDE INVENTORY OVERLAID ON TOP OF THE 2001 SUSCEPTIBILITY MAP 71

LIST OF TABLES

TABLE 1. ROCK FORMATIONS IN THE STUDY AREA. 20
TABLE 2. LAND COVER CLASSES WITH ASSOCIATED WITH SOFTWARE IDENTIFYING CODES. 30
TABLE 3. OVERALL ERROR AND KAPPA INDEX OF AGREEMENT STATISTICS FOR THREE LAND COVER CLASSIFICATION METHODS. 31
TABLE 4. BREAKDOWN OF SLOPE ASPECT WITHIN THE STUDY AREA. 37
TABLE 5A. RESULTS OF THE LANDSLIDE INVENTORY AND THE GEOLOGIC ATTRIBUTE FOR 2001. 48
TABLE 5B. RESULTS OF THE LANDSLIDE INVENTORY AND THE GEOLOGIC ATTRIBUTE FOR 2005. 48
TABLE 6A. RESULTS OF THE LANDSLIDE INVENTORY AND THE FAULT LINES ATTRIBUTE FOR 2001. 49
TABLE 6B. RESULTS OF THE LANDSLIDE INVENTORY AND THE FAULT LINES ATTRIBUTE FOR 2005. 49
TABLE 7A. RESULTS OF THE LANDSLIDE INVENTORY AND THE LAND COVER ATTRIBUTE FOR 2001. 50
TABLE 7B. RESULTS OF THE LANDSLIDE INVENTORY AND THE LAND COVER ATTRIBUTE FOR 2005..... 50
TABLE 8A. RESULTS OF THE LANDSLIDE INVENTORY AND THE ELEVATION ATTRIBUTE FOR 2001..... 51
TABLE 8B. RESULTS OF THE LANDSLIDE INVENTORY AND THE ELEVATION ATTRIBUTE FOR 2005. 51
TABLE 9A. RESULTS OF THE LANDSLIDE INVENTORY AND THE SLOPE ATTRIBUTE FOR 2001. 52
TABLE 9B. RESULTS OF THE LANDSLIDE INVENTORY AND THE SLOPE ATTRIBUTE FOR 2005. 52
TABLE 10A. RESULTS OF THE LANDSLIDE INVENTORY AND THE SLOPE ASPECT ATTRIBUTE FOR 2001.... 53
TABLE 10B. RESULTS OF THE LANDSLIDE INVENTORY AND THE SLOPE ASPECT ATTRIBUTE FOR 2005..... 53
TABLE 11A. RESULTS OF THE LANDSLIDE INVENTORY AND THE RIVERS ATTRIBUTE FOR 2001. 54
TABLE 11B. RESULTS OF THE LANDSLIDE INVENTORY AND THE RIVERS ATTRIBUTE FOR 2005..... 55
TABLE 12A. RESULTS OF THE LANDSLIDE INVENTORY AND THE TRIBUTARIES ATTRIBUTE FOR 2001..... 55
TABLE 12B. RESULTS OF THE LANDSLIDE INVENTORY AND THE TRIBUTARIES ATTRIBUTE FOR 2005. 55
TABLE 13A. RESULTS OF THE LANDSLIDE INVENTORY AND THE ROADS ATTRIBUTE FOR 2001 55
TABLE 13B. RESULTS OF THE LANDSLIDE INVENTORY AND THE ROADS ATTRIBUTE FOR 2005 52
TABLE 14. PAIR-WISE COMPARISON RATING SCALE WITH NINE DIVISIONS. 53
TABLE 15. PAIR-WISE MATRIX SHOWING CALCULATED FACTOR WEIGHTS FOR ALL NINE ATTRIBUTES. ... 56
TABLE 16. SCALED WEIGHT OF EACH ATTRIBUTE USED IN THE FINAL LANDSLIDE SUSCEPTIBILITY CALCULATION 60
TABLE 17A. THRESHOLDS AT WHICH INDIVIDUAL PIXELS WERE ASSIGNED THEIR SUSCEPTIBILITY CLASS 2001. 63
TABLE 17B. THRESHOLDS AT WHICH INDIVIDUAL PIXELS WERE ASSIGNED THEIR SUSCEPTIBILITY CLASS. 2005. 63
TABLE 18A. AMOUNT OF STUDY AREA CONTAINED WITHIN EACH SUSCEPTIBILITY CLASS 2001 64
TABLE 18B. AMOUNT OF STUDY AREA CONTAINED WITHIN EACH SUSCEPTIBILITY CLASS 2005 64
TABLE 19. SCENARIO I 2001 LANDSLIDE INVENTORY OVERLAID ON THE 2001 SUSCEPTIBILITY MAP. 69
TABLE 20. SCENARIO II 2005 LANDSLIDE INVENTORY OVERLAID ON THE 2005 SUSCEPTIBILITY MAP. 69
TABLE 21. SCENARIO III 2005 LANDSLIDE INVENTORY OVERLAID ON THE 2001 SUSCEPTIBILITY MAP. ... 70
TABLE 22. AVERAGE DIFFERENCE IN LANDSLIDE OCCURRENCE RATES FOR EACH ATTRIBUTE BETWEEN THE 2001 AND 2005. 72

I. INTRODUCTION

Azad Jammu and Kashmir (AJK), a disputed territory in Northern Pakistan, is an area located atop the Western Himalayas. Widely renowned for it breathtaking landscape, AJK is prone to large-scale disasters such as earthquakes and landslides. Landslides are one of the most widespread and damaging hazards in the Himalayas. Landslides can be particularly harmful when adjacent to human settlements and infrastructure such as towns, roads, bridges and utilities and are potentially deadly to the local populations. The high susceptibility to landslides of the Western Himalayan terrain is largely due to a complex geological setting combined with frequent seismic activity, varying slopes and relief, heavy rainfall during the monsoon season, increasing amount of human development and a rapidly growing population. In the wake of such a disaster, people of the region are looking to establish new standards in dwelling and road construction, and to develop routes for escape and make relief more accessible particularly in the more remote areas. These types of changes require complex analysis of the landscape with modern technology to ensure that the proper procedures and polices are put into effect in a timely fashion to reduce any preventable loss of life and damage of property (Saha, 2002).

1. The Earthquake

On October 8, 2005 at 8:50 am local time a devastating 7.6 magnitude (Richter scale) earthquake struck the Lesser Himalaya in Pakistan and India. The epicenter was located at 34°29′35″ N and 73°37′44″ E, just outside the regional capital of Muzaffarabad

in the Pakistani-controlled portion of Azad Jammu and Kashmir (Figure 1). The massive quake had a focal depth of 26 km and the main shock was followed by 978 aftershocks of magnitude 4.0 and higher until October 27, 2005 (EERI, 2005).

Figure 1. Location of Earthquake epicenter in Azad Jammu-Kashmir in northeastern Pakistan. (http://www.bbc.news.co.uk).

The earthquake and its many aftershocks traumatized the people and ravaged the land and infrastructure of the region, completely overwhelming this marginalized area of northern Pakistan. The 2005 earthquake event is reported as the deadliest earthquake in recent history of the sub-continent with approximately 72,800 fatalities; 68,700 injuries; and close to 400,000 buildings destroyed resulting in about 2.8 million people left homeless in Pakistan alone (Peiris et al., 2006). Figure 2 demonstrates how deadly the 2005 Kashmir earthquake was when compared with other earthquakes worldwide since 1900. High population density surrounding the epicenter of the powerful 7.6 magnitude

earthquake exacted a massive human toll. Loss of life is attributed to the earthquake itself and was exacerbated by the numerous mass movements triggered by the intense shaking.

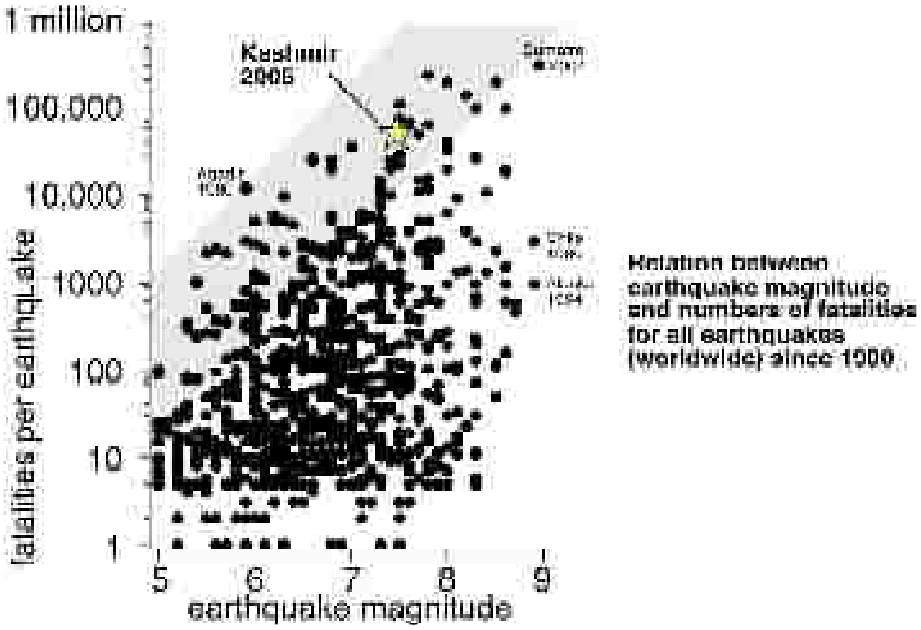

Figure 2. Fatalities in relation to magnitude for worldwide earthquakes since 1900 (CIRES 2006).

2. Objectives

The main objectives of this research are three-fold: First, to quantify the amount of landsliding immediately after the earthquake by creating a landslide inventory in a GIS environment by using field work and remote sensing analysis in an effort to evaluate the impact of the earthquake on the landscape before and after the snowmelt season; second, to develop a landslide susceptibility zonation GIS for the purposes of hazard assessment and mitigation; and third, to verify the methodology and resulting susceptibility GIS map by testing the known post-earthquake landslides against a pre-earthquake susceptibility map of the same region.

Ultimately, this study is an attempt to prepare a landslide susceptibility zonation map (LSZ) that includes portions of the Jhelum, Neelum and Kaghan valleys in the Lesser Himalaya using remote sensing and GIS technology. Landslide susceptibility zonation is a rapidly advancing methodology and that entails the ranking of different portions of an area according to the degrees of actual or potential hazard from landslides (Varnes, 1984). The LSZ produced by this study will be used to appropriate quick and safe mitigation measures and future strategic planning and identification of landslide-prone areas within the confines of the selected study area (Saha, 2002).

3. Hypotheses

This study will evaluate the following three hypotheses:

1. Rates at which landsliding occurs within the individual characteristics of each influencing attribute will remain consistent before and after the earthquake event. Frequency of landslides will increase, but the amount of influence of each attribute will remain the same.

2. Landslides occur in connection with specific localized environmental settings. The most influential attribute within the designated study will be the local geology. Land cover will also prove to be extremely important, especially on the amount of sliding that occurs post snow-melt season. Human infrastructure (roads) will have a significantly negative effect making unstable slopes adjacent to hydrologic features even more dangerous.

3. The earthquake weakened many slopes that did not succumb to failure. With the impending onslaught of the monsoon season and the spring thaw there will be a

significant increase in new and reactivated landslides. These pose a serious threat to the area for the immediate and near future making the creation of a LSZ all the more necessary.

II. BACKGROUND

1. The 2005 Kashmir Earthquake

Several studies exist that focus on the geomorphoic consequences of the Kashmir quake. Abbasi (2002) conducted a study of slope failure and landslide mechanisms in the Murree area of Northern Pakistan. Several authors focused on examining different aspects of the earthquake event using several field techniques and remote sensing technology (Avouac, 2006; Pathier, 2006; Wang, 2007; Pararas, 2007). The results of these studies often found specific information pertaining to the underlying cause of landslides in the region; for example Kumar, (2006) used remote sensing technologies to produce a geological assessment of the study area and found failures to be spatially distributed along the active faults. Other studies focused on landslides and their geomorphic, economic, and environmental effects (Harp, 2006; Kamp et al., 2008; Owen et al., 2008; Peiris, 2006; Sudmeier-Rieux, 2007; Trommler, 2008; Yeates, 2008). The result of most of these undertakings was the examination of landslides using satellite images, landslide susceptibility modeling and field research in an effort to help the local policy makers and engineers design a sustainable disaster risk reduction strategy and recovery plan.

2. Susceptibility Mapping

Landslide susceptibility mapping has been emphasized as an emerging area of worldwide research starting in the late 1980's. Multiple analytical techniques have been developed since then in nearly every major mountain chain (Brabb, 1984; Carrara, 1991,

1992; Pachauri, 1998; Chung, 1999). Evolving technology and a growing need for landslide hazard data in times of crisis has spurred even more research in recent years (Barredo, 2000; Ayalew, 2004; Saha-Gupta, 2005; Akgun, 2007; Remondo, 2008; Zezere, 2008). Several susceptibility and hazard mapping studies have been carried out for the Himalayas (Anbalagan, 1992; Pachauri and Pant, 1992; Gupta et al., 1993; Virdi et al., 1997).

Landslides are a form of a natural hazard. By definition a natural hazard is "a source of danger to life, property, and the environment" (Abbot, 2004:445). Areas that are susceptible to landslides, but are not in proximity to any human infrastructure, would not be considered a hazard. The city of Muzaffarabad and surrounding valleys have an extremely high population density and an extensive infrastructure, so any landslide mapping done in this area should be considered hazard mapping. Hazard mapping involves a temporal framework and attempts to predict frequency and spatial distribution of future slope failures over a specified period of time. The term landslide susceptibility map and landslide hazard map are often used as interchangeable terms in recent studies. Owing to conceptual and operational limitations, most landslide hazard maps could be better defined as landslide susceptibility maps (Brabb, 1984). This study does not predict over any temporal periods; therefore it will produce only a susceptibility map.

"In its very simplest form landslide maps provide information about the spatial distribution of landslides in relation to certain controlling factors" (Asch, 1984:40). These controlling factors vary in number and influence for each individual area of study. Once these parameters are factored in, the area is divided into zones or degrees of susceptibility to create a landslide susceptibility zonation. According to Van Westing

(2003: 399), “The term zonation in a general sense implies a division of the land into areas and their classification according to degrees of actual or potential landslide hazard or susceptibility”. The areas of the map divided into zones in order to simplify and improve the maps readability so that it may reach a broader audience. Upon completion, the susceptibility zonation map should communicate the potential danger of future landsliding at any given point or area.

Landslide susceptibility mapping might follow a qualitative or quantitative approach. The latter includes deterministic or statistical methods, which often involve large amounts of input data concerning the geotechnical parameters and require complex methods to acquire and process the vast amounts of information. Hence, they are best suited for site specific research or individual failures and not a regional analysis (Fall, 2006), such as the one being undertaken in this study.

The qualitative approach includes the heuristic method, which uses either direct or indirect mapping. Direct mapping analyzes the degree of susceptibility either in the field or immediately upon completion of the field work; it is reserved for small scale mapping and usually includes complex groundwater data. Indirect mapping utilizes data integration techniques, including qualitative methods, in which the researcher can assign weighted values to a series of geomorphologic- and human-induced parameters to each class within each parameter. The parameter layers are then interpreted within the GIS to produce susceptibility values (Barredo et al., 2000). Each of the characteristics is assigned a weighted value according to the relative influence it has in triggering a mass movement. Several methods of weighting and ranking have been developed such as the analytic hierarchy process (AHP), weighted linear combination (WLC), bivariate (BSA)

and multivariate statistical analysis (MSA), stepwise discriminate analysis, and logistic regression (Ayalew, 2005).

3. Landslide Classification

There are many different types of landslides characterized by movement and material (Varnes, 1978). The types of movements are categorized into three main classes of falls, slides and flows. The material itself is also separated into three different types of rock, debris, and earth. Each type of material is subject to each category of movement making nine total combinations possible. In rock falls, a mass, usually large boulders or rocks, becomes detached from steep slopes and descends, mostly through the air. Slides are defined as a type of mass movement in which a section of the slope weakens and separates from the more stable underlying material. There are two subcategories of slides: rotational and translational. A rotational slide is curved concavely, and the material rotates as it falls as if on an axis. A translational slide moves down slope as if on a flat plane with little rotation. A flow is usually associated with material that has a high concentration of water, and the movement can have a wide range of speed and size. Debris flows usually consist of loose soil, rock, and organic material mixed with water; they are also commonly known as mud slides. Earth flows usually occur in fine-grained silt, clay and clayey sand.

In November 2005 approximately one month after the earthquake Owen et al (2008) examined and photographed 1,293 slides at 174 locations in the study area. A landslide inventory was constructed and the slope failures grouped into six geomorphic-geologic-anthropogenic settings. These includes (i) mainly rock falls in highly fractured

carbonate rocks comprising the lowest beds in the hanging wall of the likely earthquake fault; (ii) mostly rock falls and rock slides in Tertiary siliciclastic rocks along antecedent drainages that traverse the Hazara–Kashmir Syntaxis; (iii) natural failures in high and/or fluvially incised steep (50–60°) slopes comprising Precambrian and Lower Paleozoic rocks; (iv) mostly small debris falls in very steep (N60°) lower slopes of fluvially undercut Quaternary valley fills; (v) many small rock falls and shallow rock slides on ridges and spur crests; and (vi) failures in locations associated with road construction that traverse steep (N50°) slopes (Owen et al. 2008). For the purposes of this study, the locations above were revisited and re-photographed during the months of May and June; 2006. These definitions and settings are used to classify landslides within the study area that are identified via field work and satellite interpretation. Although the different forms of mass movement have different destructive magnitudes, they are all potentially hazardous and shall all be included in the landslide inventory map. It is important to note the most probable type of slide in conjunction with the potential for slope failure, because it gives the administrative body an improved outlook in the development of future infrastructure.

III. STUDY AREA

The study area is in Azad Kashmir ("Free Kashmir"), which is the Pakistani administered section of the state of Jammu and Kashmir. This area lies within a single ASTER (Advanced Spaceborne Thermal Emission and Reflection Radiometer) satellite image[1]. The north, east and southern boundaries of the study area coincide with the satellite's boundaries, while the western boundary follows a ridgeline just west of the GPS points collected in the field. The area further west of this ridgeline does not contain any ground truthing data and was omitted from the study. In addition to the lack of ground control points, the areas west of the ridgeline contained large amounts of flat agriculture land which were not prone to earthquake-triggered landslide activity and did not require the attention of this research. The study area has a perimeter of 228 kilometers and encompasses an area containing 2,549 square kilometers of mostly rugged mountainous terrain.

The study area contains several major areas of devastation in part due to the close proximity to the earthquakes epicenter and some of the major fault lines in the area. Some of the more devastated urban areas, such as Balakot, Hattian, and Muzaffarabad are located within the boundaries of the selected research area. Muzaffarabad is of particular interest being the capital of the Pakistan controlled Azad Kashmir, only about 50 kilometers from the Pakistani-Indian Line of Control. The city is positioned on the confluence of the Neelum and Jhelum rivers. It occupies mainly gentle slopes, although it extends into the surrounding mountainous terrain. To the west of the region lies the North Western Frontier Province (N.W.F.P.). There are three principal valleys in the

[1] Bounding Coordinates: 34° 41' 37" N, 73° 53' 38" E, 34° 4' 51" S, 73° 21' 2" W.

study area: the Khagan Valley running at a NNW course from Muzaffarabad; the Neelum Valley running at a NNE direction from Muzaffarabad; and the Jhelum Valley east of Muzaffarabad running towards the India/Pakistan border (Figure 4).

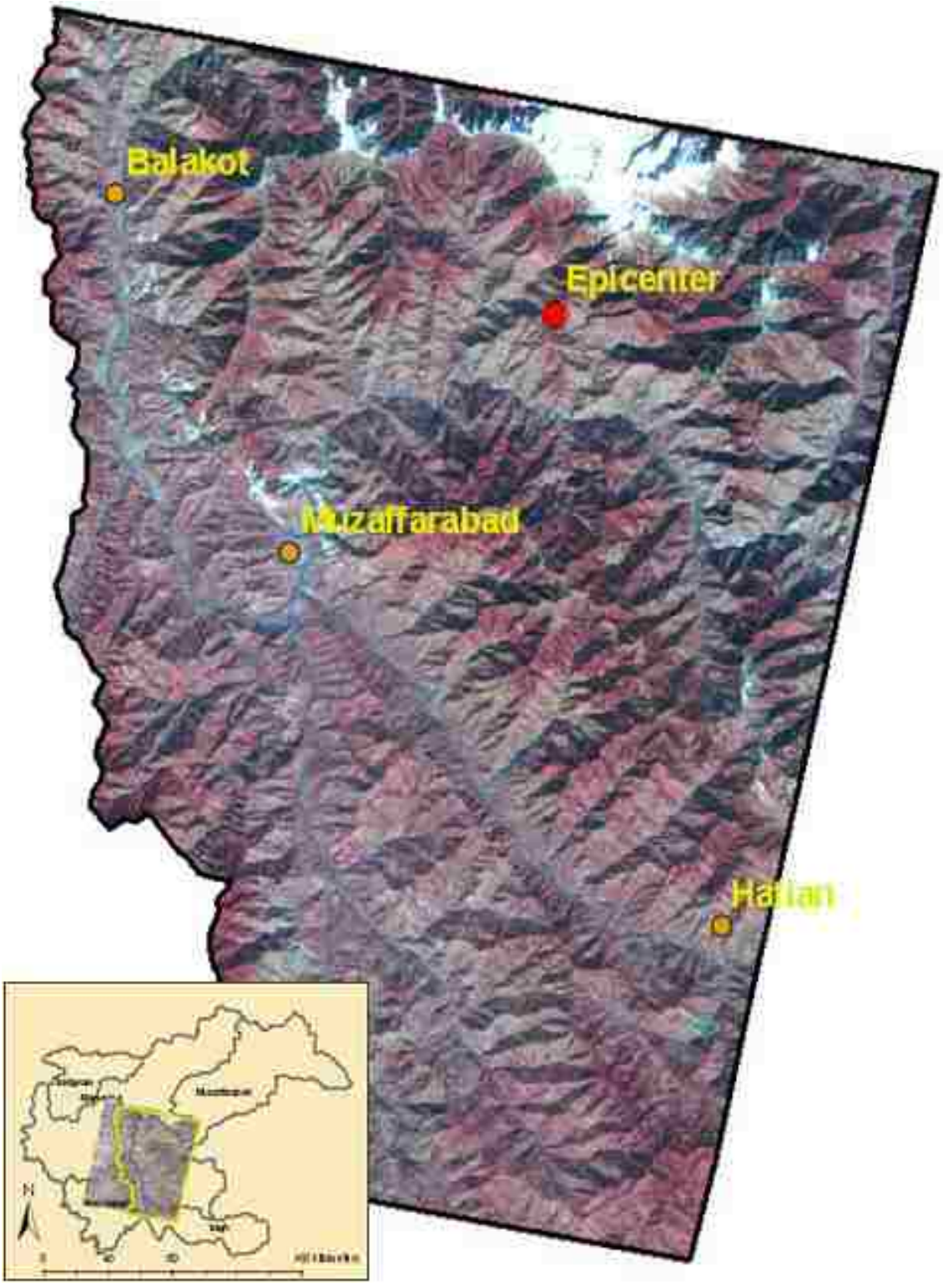

Figure 3. ASTER satellite image of the study area in northeastern Pakistan with major urban centers and earthquake epicenter.

Figure 4. Oblique three-dimensional view of study area. (Google Earth).

The total population for Azad Kashmir is over 3.2 million people with a density of approximately 252 people per square mile. There is over 750,000 living in the Muzaffarabad district alone, 80,000 of which living within the city itself (Pakistan Statistics Division, 2006). This is an extremely high population density and is the prevailing trend for the immediate areas within and surrounding the study area. In fact, the Azad Kashmir alone would rank fifth in density if it were a U.S. state.

The study area is a very complex climatic region and is often characterized as a subtropical highland climatic zone. The mountainous terrain make many different types of weather possible based on elevation, latitude, and exposure. Mean temperatures are very hot in summer (26°C) and cold in winter (6°C). Temperature usually decreases about 6.5°C for every 1000 meters of elevation. A monsoon season usually hits in late

June and lasts through August, often causing severe flooding and violent debris flows. These three months alone constitute 45 percent of the total annual rainfall of 1527 millimeters (WMO, 2006). The high steep slopes accumulate snow in winter and then shed the snow in late spring making them highly susceptible to freeze-thaw weathering and additional weakening of the slopes. Due to the rugged terrain and the varying weather extremes, travel within this region is extremely difficult (Figures 5 and 6).

Figures 5 and 6. Earthquake-triggered landsliding along road.

Along this steep environment, roads are cut into the hillside removing the material from the side of the hill. The hill slope is left in a weakened condition since it no longer has the base material to support it. Buildings and other structures are often built adjacent to these roads and usually require further cuts into the slope.

IV. METHODOLOGY

1. Field Work

The field work done in this research involves the method of repeat photography and was a continuation of previously conducted research. This previous research was carried out in November, 2005 by colleagues[2] approximately one month after the earthquake. During this earlier field campaign, an inventory of 161 landslide locations were photographed and described, including vital geomorphologic information and Global Positioning System (GPS) measurements of each location (Owen et al., 2008). Approximately six months later in late May/early June, 2006 the same study area was revisited to repeat all photographs of the existing inventory and evaluate all potential changes in each location. Information was recorded in field books and then manually put into a field computer along with the pictures on a daily basis. Both inventories from 2005 and 2006 were compared and analyzed with a focus on landsliding frequency, intensity and spatial distribution within the study area. The data from the field work proved to be invaluable ground truth information for the landslide susceptibility mapping.

2. Geographical Information System

A Geographic Informational System (GIS) offers a technological framework for supporting efficient and effective data capture, storage, management, retrieval, analysis, integration and display (Guzzetti et al., 1999). The manipulation and analysis of data can be much more efficiently and cost-effectively accomplished by applying GIS technology

[2] Ulrich Kamp and Jennifer Parker Hamilton (University of Montana); Lewis Owen (University of Cincinnati); and Ghazanfar Khattak (University of Peshawar).

as opposed to a manual field collection approach (Carrara, 1999). This study employs ESRI's ArcGIS 9.2 using a UTM Grid, zone 43N and the WGS 84 (World Geographic System) reference system. The GIS will be composed of a base map of the study area with all the identifiable landslides digitized into polygons. This landslide base map is then overlaid with the base maps for geology, vegetation, slope, human factors (construction, road cuts, land use such as forestry and agriculture) and several other characteristics. Data was analyzed and interpreted by overlaying all the layers together. The data needed was derived from satellite imagery, fieldwork, and existing topographic and geological maps.

The attributes layers produced in this study include vector (geology, faults, rivers, tributaries, roads) and raster layers (elevation, slope, aspect, land cover).

3. Susceptibility Mapping

Once the variable data is defined and collected, it must then be ranked and weighted. The scale is weighted for the reason that some elements such as geology are much more influential in slope failure. In this study, indirect mapping, an expert driven approach of weighting and ranking, was utilized since it is best suited for the amount and type of data available, the extent of the study area, and a geomorphological analyses aimed at the recognition and correct interpretation of the factors that control landslide occurrences (Casagli, 2004). The weighting and ranking system chosen is the multi-criteria, Analytical Hierarchy Process AHP method as it is incorporated within the IDRISI software used in the analysis. AHP breaks down a complex decision based

problem into a hierarchy of more easily recognizable sub-problems, each of which is then evaluated separately. This process is explained later in the thesis.

V. LANDSLIDE INVENTORY MAPS

Previous studies have indicated that it is now becoming generally accepted that susceptibility mapping starts with the inventory of landslides (Ayalew, 2004). A field survey is the most accurate method available for collecting complete landslide inventory data; however the logistics of traversing mountainous terrain such as in Azad Kashmir is difficult at best and often times due to slope instability was dangerous or impossible. Instead, the use of remote sensing technologies such as satellite imagery was used to obtain significant, cost-effective data on the size and spatial distribution of slope failure in the area (Lee, 2001).

In the pre-earthquake satellite image 28 landslides were identified and digitized as training sites, while in the post-earthquake satellite image 40 landslide sites were collected using GPS points and photographs acquired during field work. Additional landslides were then identified using Feature Analyst which identified landslides based on multiple spatial attributes (size, shape, texture, pattern, spatial association, and shadow). Results of this landslide identification were compared with existing field data. This procedure was repeated four times; the last step was a manual editing.

The pre-earthquake analysis showed 371 landslides with a combined area of ~ 8.3 km² and a mean landslide area of 0.02 km². The post-earthquake image yielded 2252 landslides comprising an area of ~ 60.8 km² and a mean landslide area of 0.027 km².

VI. ATTRIBUTE MAPS

Landslide susceptibility mapping has been a rapidly evolving area of research over the past 10 years. There are, however, many obstacles and pitfalls in the production of the individual layers, as well as the final map that impede a quick and accurate product. The primary dilemma in this study was the availability and reliability of digital data. Two pieces of GIS data (roads and tributaries) were made available through the United Nations, but were found to be noticeably inaccurate at a scale of 1:100,000 or larger and required a great deal of modification. The GPS points were collected in the field, and then downloaded and placed in the correct projection of UTM coordinates, Zone 43N. Several attributes including slope, aspect and elevation were derived from an ASTER digital elevation model (DEM) of the area using the *Spatial Analyst* extension in ArcMap 9.2. Rivers, geology, and fault lines were digitized from hardcopy maps, fifteen meter ASTER[3] satellite imagery, and (only for some locations) one meter Quickbird satellite imagery. The land cover map was created from the ASTER satellite imagery using IDRISI Andes software.

1. Geology

Geologic information was obtained and digitized from varying map sources produced by the United States Geological Survey (USGS), the Geological Survey of Pakistan, and the United States Agency for International Development (USAID).

[3] Jeff Olsenholler from the Department of Geography and Geology at the University of Nebraska - Omaha generated and orthorectified the ASTER DEMs using SILCAST software.

Attribute table generation followed the same symbology found in the original data sources.

The bedrock underneath the study area is comprised of eleven different formations, three of these, the Murree, Hazara and Salkhala formations, dominate approximately 73% of the area (Table 1; Figure 7). The Jhelum Valley consists almost exclusively of the Murree Formation with the very end of the valley peaking into the Panjal Formation. The Neelum Valley passes through the Kingriali Formation and then secondly into the Murree Formation. The Khagan Valley consists of the Hazara Formation before traveling NNW including pieces of the Panjal and Salkhala formations.

Table 1. Rock formations in the study area.

Valley	Formation	% of Study Area	Lithology
JHELUM	Kamlial	8.09	Grey to red sandstone and shale mixed with some conglomerate
	Murree	51.52	Red, thin-bedded shale, mudstone and greywacke
	Panjal	3.11	Agglomeratic slate
	Samana Suk	0.15	Limestone
	Kawagarh Limestone	0.16	Marl, shale, and limestone
NEELUM	Kingriali	2.91	Dolomite, limestone, conglomerate, quartzose sandstone, siltstone
	Salkhala	13.66	Limestone and marble
	Manshera Granite	5.70	Intrusive rock; granite
KHAGAN	Hazara	11.13	Black slate, shale, siltstone, graphite, limestone
	Tanawai	1.58	Quartzose schist and quarzite
	Panjal	3.11	Agglomeratic slate
	Alluvium	1.97	Alluvium

The Murree Formation has an overwhelming presence (~ 52%) within the study area. It includes red thinly laminated siltstone and shale, thick-bedded red mudstone, and subordinate green, gray, and maroon greywacke (Calkins et al., 1975). An exact age is

difficult to obtain, however, most experts believe the formation to be from the Tertiary age probably from the Miocene or Oligocene epoch.

The Salkhala Formation represents some of the oldest known rocks in the region consisting of mainly metamorphic rocks from the Precambrian age. Within the study area the Salkhala Formation has a strong presence in the north-east portion of the study area and is bordered by units of Manshera Granite and the Murree Formation. It consists largely of quartz schist, marble, graphite schist, and quatrzo-feldspathic gneiss (Calkins et al., 1975).

The Hazara Formation is composed of slate, phyllite, unmetamorphose shale and some limestone and graphite. This formation has a substantial presence within the southwest portion of the study area and is located in the Muzaffarabad vicinity and to the area directly south.

The Kamlial Formation represents a small portion in the NW of the study area, adjacent to the Kingriali and Murree formations. It consists primarily of grey to brick-red medium to coarse grained sandstone interbedded with purple shale and an intraformational conglomerate (Kazmi, 1998). Its age is thought to be middle to late Miocene.

Manshera Granite is not a formation like the preceding geological units but rather a large unit of intrusive rock found commonly along the southern fringes of the granite intrusions of the Himalayan region. The granite is light colored and is usually found to be medium to course grained. The age of the rock is inconclusive as the youngest rocks intruded belong to the Tanawal Formation of Ordovician to Devonian periods (Calkins et al., 1975).

The Panjal Formation contains agglomeratic rock that consists of slate or shale, glassy quartzose agglomeratic sandstone and small amounts of phyllite and conglomeratic sandstone. In western Kashmir it is thought to range from Carboniferous to Permian in age (Calkins et al., 1975). The Panjal Formation runs right along with the Panjal Thrust and the Main Boundary Thrust (MBT) and is also found in the northwest portion of the study area near Balakot.

The Kingriali Formation consists of grey dolomite and dolomitic limestone with dolomitic shale and marl and is believed to be late Triassic in age (Kazmi, 1997). The formation area located within the study area has also been known to contain small amounts of quartzite and phyllite. In the massive response to the 2005 earthquake, an inconsistency arose in the nomenclature of the formation with new studies referring to the unit as the Muzaffarabad Formation, probably due to the location as it runs between the two towns of Muzaffarabad and Balakot. The two names shall be considered interchangeable as the reference the exact same formation.

The Alluvium in the region represents quaternary deposits which are stream-deposited sand, gravel and boulders. Patches are found near or juxtaposed to current or ancient stream beds and are now used for terrace farming, particularly around Muzaffarabad and also north and east of the city.

The Tanawai or Tanawal Formation is a subset of the Kirana Group and consists mainly of quartzose schist and quartzite (Kazmi, 1997). The formation is thought to range in age from the Ordovician to Devonian period with and is composed of 70-90% quartz schist (Calkins et al., 1975). Within the study area the Tanawai Formation appears

in the Khagan Valley running a NW-SE direction and is situated in-between long segments of alluvium and Manshera Granite.

The Samana Suk limestone and Kawagarh limestone units represent only a small portion (0.3%) in the western part of the study area. The Samana Suk limestone contains black to dark gray thick-bedded limestone, while the Kawagarh limestone is light gray, but is commonly stained in shades of brown or red because of the presence of limonite and siderite (Calkins et al., 1975). Calcareous shale and dark marl also are found within the Kawagarh Formation. Samana Suk limestone is thought to be Jurassic in age while the Kawagarh limestone is younger and is thought to be of late Cretaceous age.

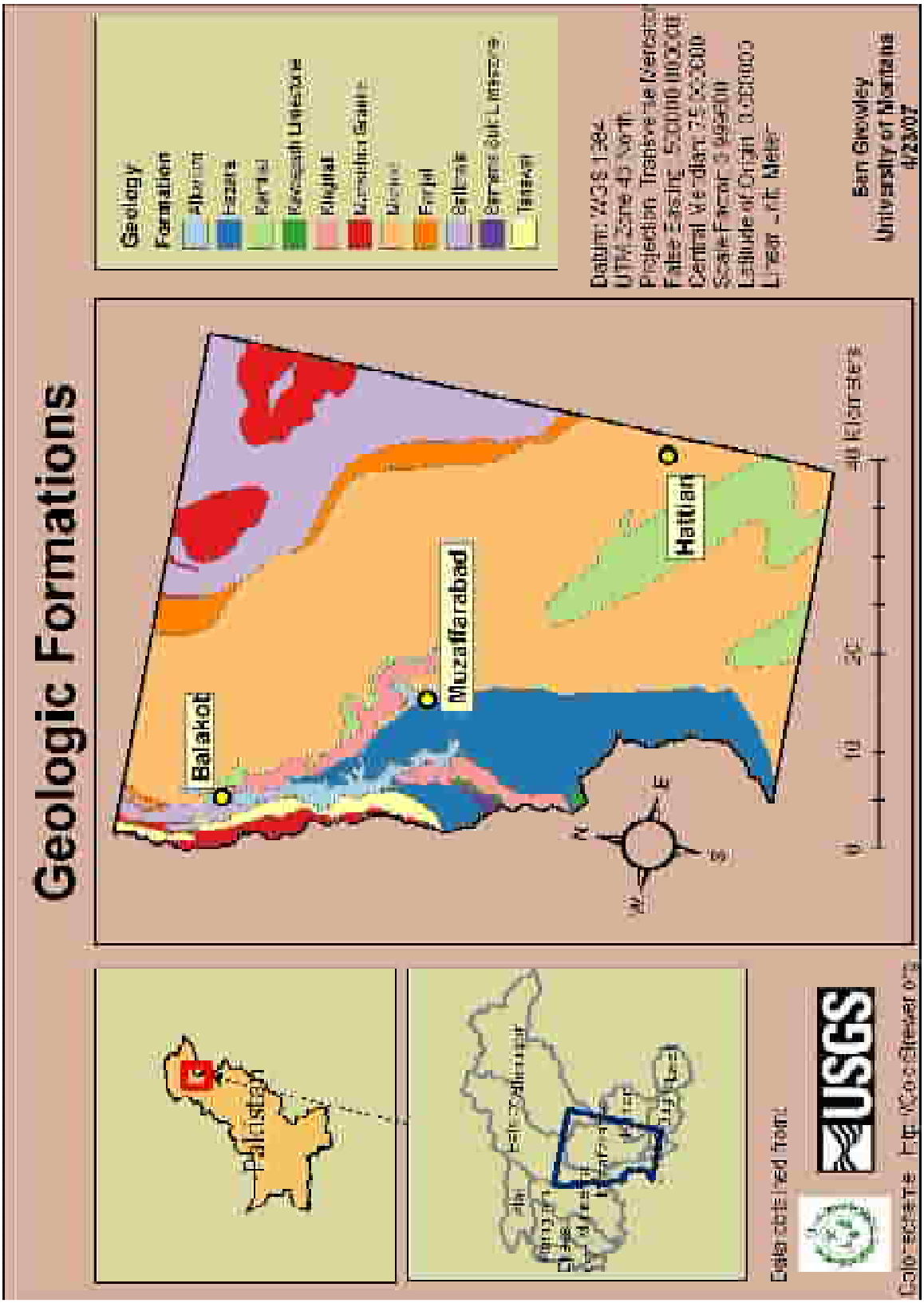

Figure 7. Geologic map of the study area.

2. Faults

The faults attribute layer was digitized from the same sources as the geological layer. Appropriate symbols and labels were then added to produce the final result as seen in Figure 9.

Several major active fault systems traverse northern India and western and northern Pakistan. The earthquake occurred along the Hazara-Kashmir Syntaxis, a tectonic boundary which is historically characterized by high seismic activity. Within this boundary, geological formations and the broader geological structures of the Himalayas make an abrupt bend (Kazmi, 1998). The syntaxis was formed by the interactions of the Indian, Arabian and Eurasian plates. The Indian plate moves in a northward direction at a rate of about 40 mm/year (Pararas, 2007). Compression along these boundaries results in thrust and reverse faults often resulting in colossal amounts of deformation of the terrain and destruction of human infrastructure. The area surrounding Muzaffarabad and extending to the NW is known as the Indus-Kohistan seismic zone and is host to a number of earthquakes in the last 100 years (Figure 8).

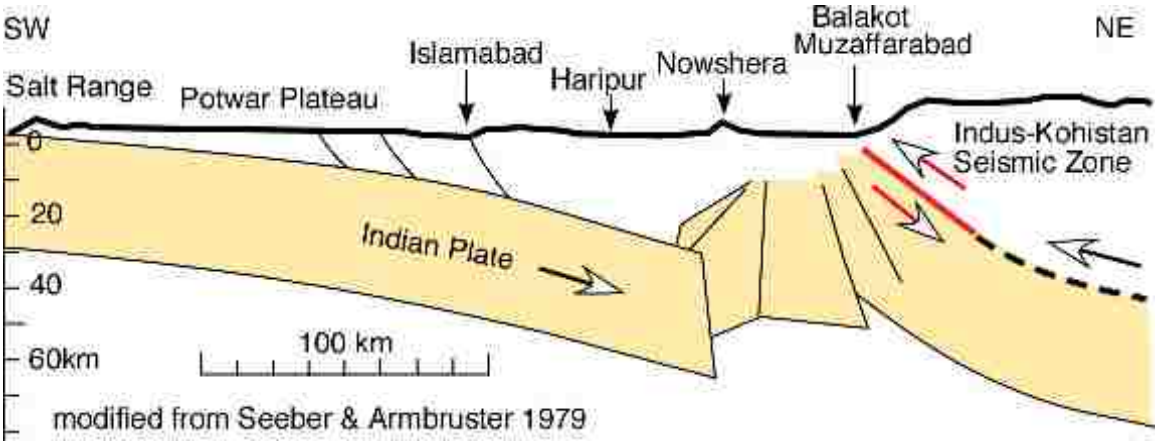

Figure 8. Profile of collision zone between Indian and Eurasian plates with Indus-Kohistan seismic zone (Bendick et al., 2007).

The October 8, 2005 earthquake occurred near the Main Boundary Thrust (MBT), a region of major tectonic plate collision that includes Northern Pakistan. Its focal mechanism and slip-strike components are consistent with the compressive type of thrust faulting which is characteristic of the Hazara-Kashmir Syntaxis (Pararas, 2007). The MBT is clearly evident within the study area (Figure 9) as it incorporates the Jhelum Fault and the Muzaffarabad Fault on the western portion of the study area and the Panjal and Parachinar faults (also known as Murree-Parachinar Fault) in the east. Another major fault in the study area, the Balakot-Bagh Fault runs right through the city of Muzaffarabad from the north and then southeast down the Jhelum Valley. The Balakot-Bagh Fault or Kashmir Boundary thrust (KBT) is primarily responsible for the Hattian landslide[4]. A buffer zone of 300 m surrounding the fault lines was reported as seeing the most uplift and landsliding activity (Hussain, 2006), while almost all mass movement occurred within a 10 km buffer zone of the fault lines. Synthetic Aperture Radar (SAR) data showed a 90 km-long belt of deformation along the KBT (See Figure 9). This deformation had a vertical displacement of greater than 1 meter, with uplift as great as 6 meters (Fujiwara et al., 2006). This extreme and rapid upheaval originating from fault lines causes many hill slopes to weaken and/or fail.

[4] Large sturzstrom that occurred near the town of Hattian 40km SE of Muzzafarabad in the Jhelum valley. Head to toe measured 2.9 km and had an estimated volume of 1-2 million cubic meters (EERI, 2005).

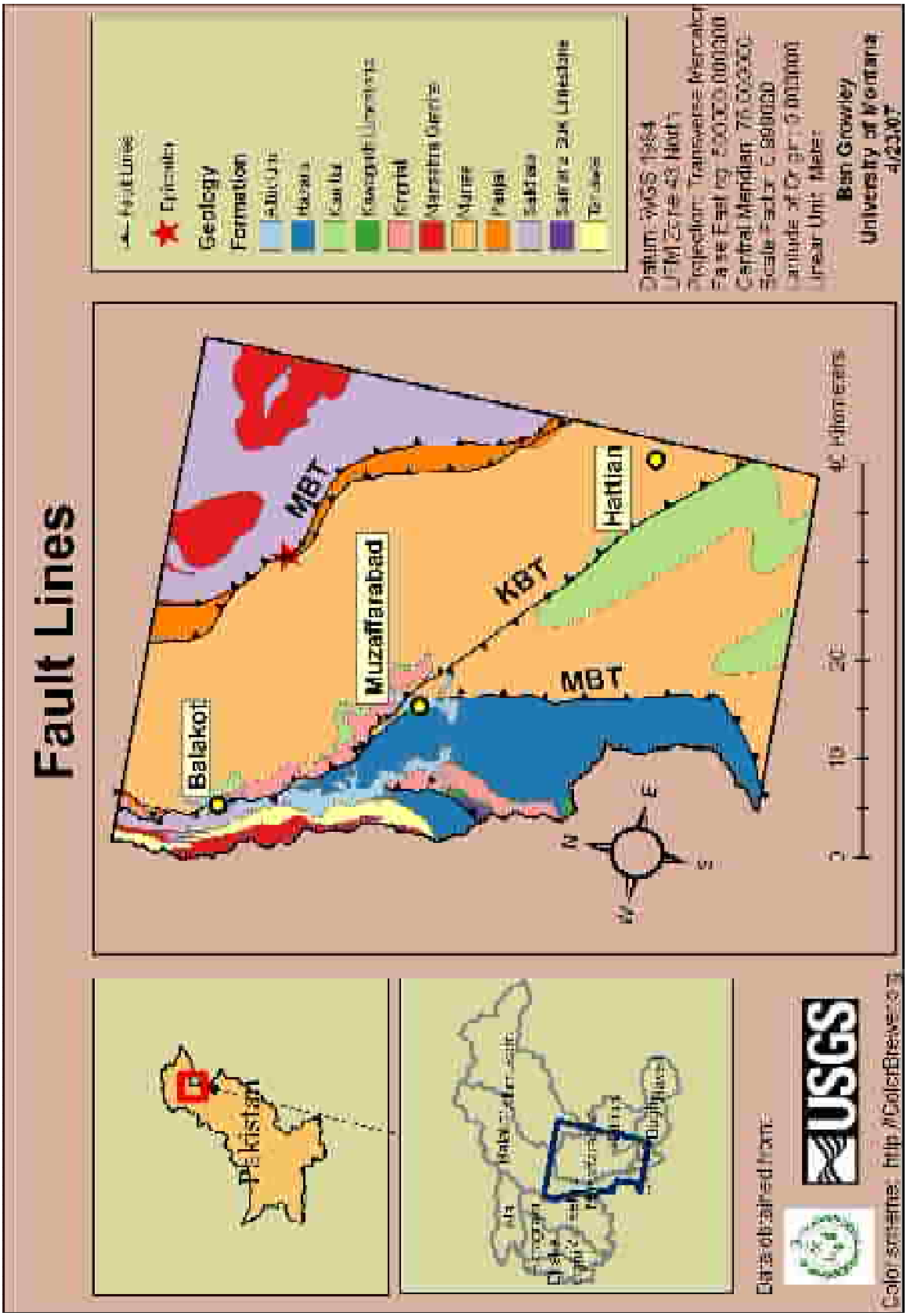

Figure 9. Fault lines within study area.

3. Land Cover

The land cover attribute was the most intricate and complicated layer to produce. Images were first needed to be converted from an ESRI grid to a format that was readable by the IDRISI software to produce a land cover classification. Eight classes were created representing the various land cover types found within the study area. They include: water, urban[5], snow and ice, forests, shrub land and grassland, agriculture, and two landslide type categories. The landslide classes were necessary since there was extensive pre-existing and post-earthquake failures that represented a substantial portion of the image. The failures occurred in different lithological settings which produced different spectral signatures. Thus, two landslide categories were identified: (1) landslides occurring in and around the Muzaffarabad area, which contain mostly alluvium and dolomite causing a very high reflectance resulting in a white chalky appearance in the ASTER image; (2) landslides occurring mainly in the Murree Formation which gave pixels a lower reflectance value that appeared light blue. Finally, these two landslide classes were consolidated into a single category and are displayed as "unclassified" in the final maps.

Several supervised classification techniques are provided by the IDRISI software such as: Parallel-piped, Maximum Likelihood, Fisher, and several neural network methods. One such neural network method, Multi-layer Perception (MLP) produced the best overall results when compared with the Maximum Likelihood and the Fisher techniques.

[5] Urban areas were detected when dense amount of infrastructure and people were located in a common area giving a pixel reflectance of light to medium blue.

Several training sites were created for each of the eight land cover classes using field data that included GPS points, field book notes, and photographs. The training sites were digitized and assigned a code number (1-8) so the software could identify each pixel with a number (Table 2). This assigned a spectral signature to each class and allowed the classes to be set with a qualitative palette for easy identification. Generally, there should be 10 times as many pixels for each training class as there are bands in the image to classify (Akgun, 2005). Thus, more than 80 pixels were used per class in the creation of the training sites. After the training sites were established, the MAKESIG operation in IDRISI was used to create the signature files, which contain the statistical information about the reflectance. Once the signature files were created, it was then possible to test the three different land cover classifiers.

Table 2: Land cover classes with associated with software identifying codes.

Class	**Code**
Water	1
Urban	2
Snow/Ice	3
Forests	4
Shrubs/Grassland	5
Agriculture	6
Landslide Type 1	7
Landslide Type 2	8

After the creation of the eight land cover classes, accuracy assessments were done for each of the three classifiers (Maximum likelihood, Fisher, MLP). The first step in this process was to identify random points to use as the ground truth points for the classification. Twenty-six random points were chosen as ground truth locations from

among the 161 GPS points in the study area. Each of the GPS points is accompanied by pictures from two different post-earthquake dates which were then used as ground truth mechanisms for each of the 26 points. Each point was digitized in IDRISI by locating the exact pixel that contained the GPS coordinates found in ArcGIS 9.2. Normally, the point would be marked with exact coordinates, but due to a technical problem, this pixel technique was substituted as an acceptable alternate method. The points were then digitized at an estimated distance from the picture location using the angle that was included in the metadata. Once this was complete, the vector layer containing the 26 points was converted into a raster layer and then assigned as the feature definition file. The ERRMAT procedure was then run using that definition file on each of the land cover classifications. A table containing commission, omission and overall errors was produced. The Kappa (Index of Agreement) values were automatically calculated for upon the completion of each technique (Table 3). These Kappa values indicate a statistical measure of inter-rater reliability for each method.[6]

Table 3: Table showing overall error and Kappa index of agreement statistics for three land cover classification methods.

Classifier	Overall Error	Kappa Value
Maxlike	0.3615	0.6408
Fisher	0.4000	0.5878
MLP	0.2837	0.6678

In this study, the MLP method was chosen for the final land cover classification since it produced the best results. The MLP network is trained with a back propagation or related learning algorithm, which is frequently being used for image classification

[6] Kappa values less than 0.00 have a less than chance agreement, values between 0.00-0.20 have a slight chance, 0.21-.0.40 a fair chance, 0.41-0.60 a moderate chance, 0.61-0.80 a substantial chance and values between 0.81-1.00 an almost perfect chance of agreement (Landis and Koch, 1977).

(Day, 1997). MLP consists of a set of simple processing units arranged in a layered architecture that can, once trained, transform the remotely sensed data into the desired classification. The number of input and output units is determined by the characteristics of the remotely sensed data to be classified and the desired classification scheme (Foody, 2004). Each unit or pixel is connected by a weighted connection. Once the analysis starts, the method runs through a series of iterations which take the found error and passed backwards through the network with the weights connecting the units adjusted in relation to the magnitude of the calculated error.

Multiple trials were conducted using the designated training sites to attain the best overall accuracy. The best trial ran through 2,390 iterations giving an accuracy of 71.63 %[7]. In the study area, the three classes "Forest" (45%), "Shrub land and Grassland" (~42%), and "Agriculture" (6.4%) dominate the landscape (Figure 11). The "Water" class (1.4%) includes only rivers since no large lakes exist. "Snow and Ice" (1.1%) can be found only in the north, where no field GPS points exist. "Urban" areas (0.5%) are mainly constituted along the rivers, and three larger urban areas exist within the area: Muzaffarabad, Balakot, and Hattian. The results of our land cover classification closely parallels that of the AJK Forest Department (2001), which defined 42% forest, 42% uncultivable land mainly for grazing, 13% cultivated land and 3% urbanized area.[8]

[7] Thomlinson et al. (1999) set a target of an acceptable overall accuracy of 85% and no less than 70%.
[8] Area in AJK Forest Department (2001) is not identical to the study area of this thesis. Study area is included within and represents approximately 20% of AJK.

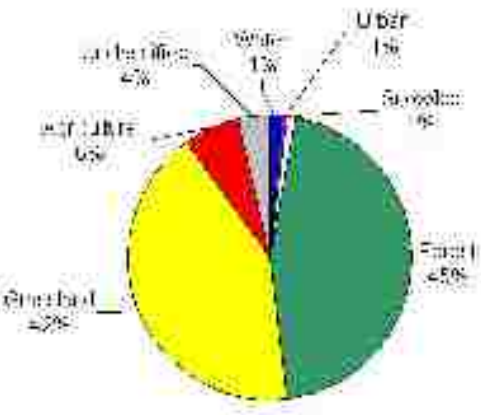

Figure 10: Land cover distribution within study area.

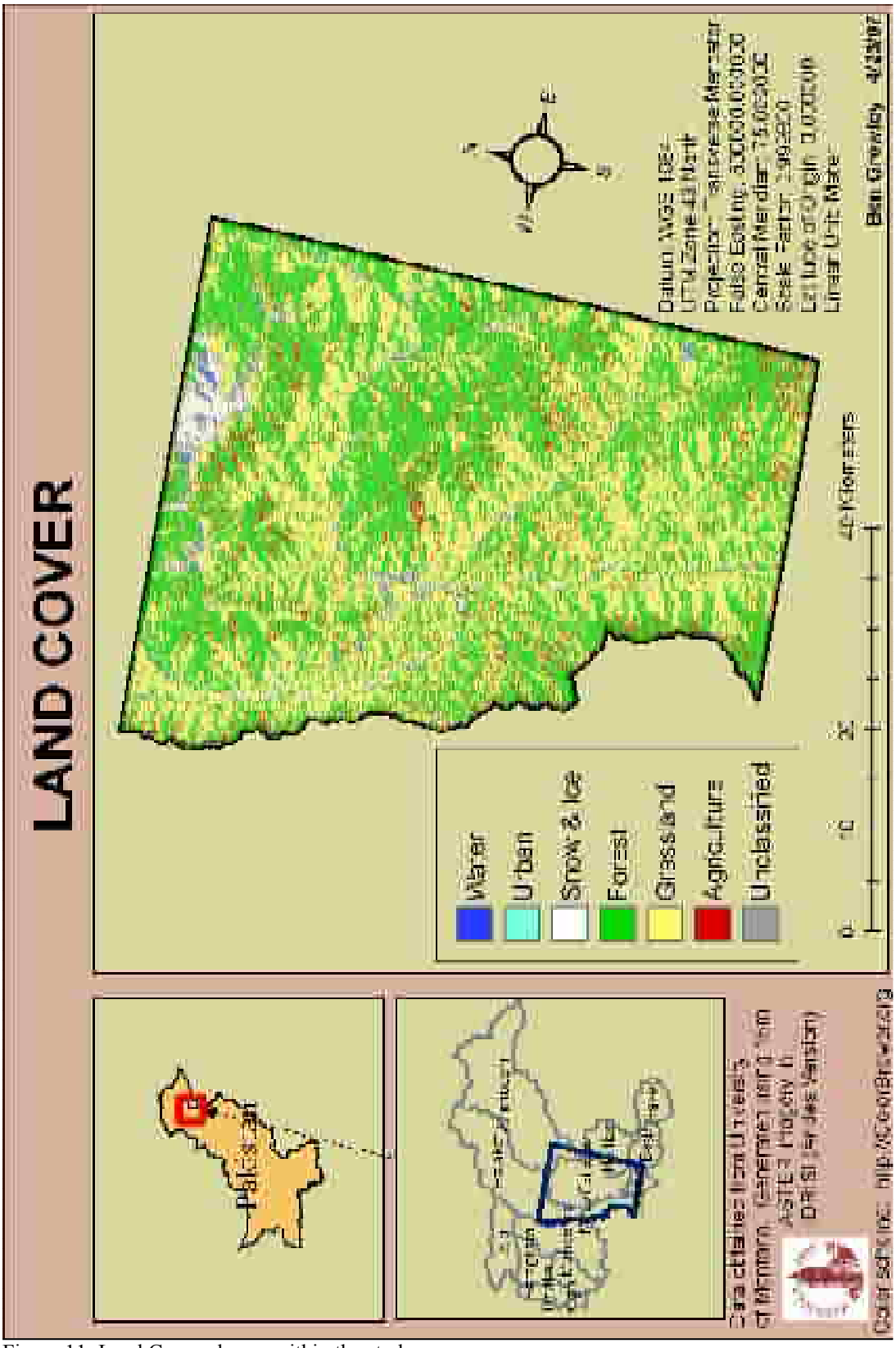

Figure 11: Land Cover classes within the study area.

4. Elevation

The attributes elevation, slope, and aspect were derived from the 15 m ASTER DEM using SPATIAL ANALYST in ArcMap. Elevation in the study area ranged from 447 meters asl. mainly in river beds and surrounding flood plains to 4,446 m in the north central portion of the region. A contour map with 500 m intervals was generated from the DEM. The majority (54%) of the study area lies between 1,000 and 2,000 m asl; 28% lies between 2,000 and 3,000 m asl; only 12% is at an elevation of < 1,000 m asl; and a small portion (~ 6%) is higher than 3,000 m asl. (Figure 12).

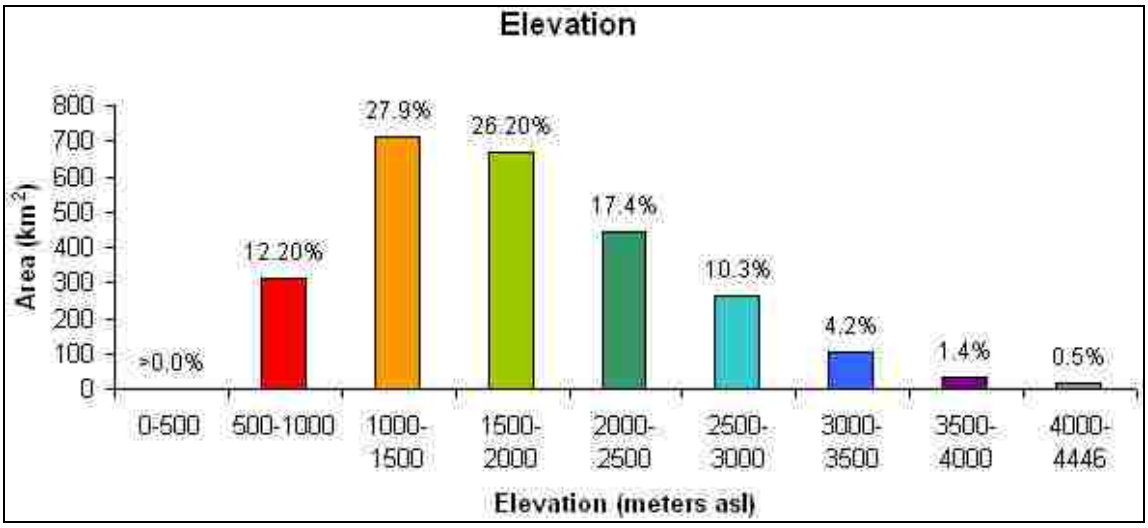

Figure 12: Bar graph indicating a percentage breakdown of elevation within the study area at 500 meter contour interval.

5. Slope

Slope is one of the most important factors in mass wasting (Ayalew, 2004; Lan, 2004; Neuhauser, 2006). There is an understandable and obvious link between slope and landslide activity. Movement occurs when slopes are steeper than the natural angle of repose of the material. The angle of repose is the steepest angle that a slope can maintain

without failing, and is typically 25-40 degrees for unconsolidated materials. The average slope for the study area is 16 degrees. The majority (31%) of all slopes falls within the range of 25 and 35 degrees, while only very few (~2%) of the area has a slope > 45 degrees (Figure 13). Nearly a quarter (22%) of all land has gentler slopes of < 15 degrees. Most of the lands with gentle slopes are utilized as urban or agricultural areas, including valley bottoms and slope terraces. Slopes with angles of 25-35 degrees were the most susceptible to landsliding with 41% of all failures occurring within that range.

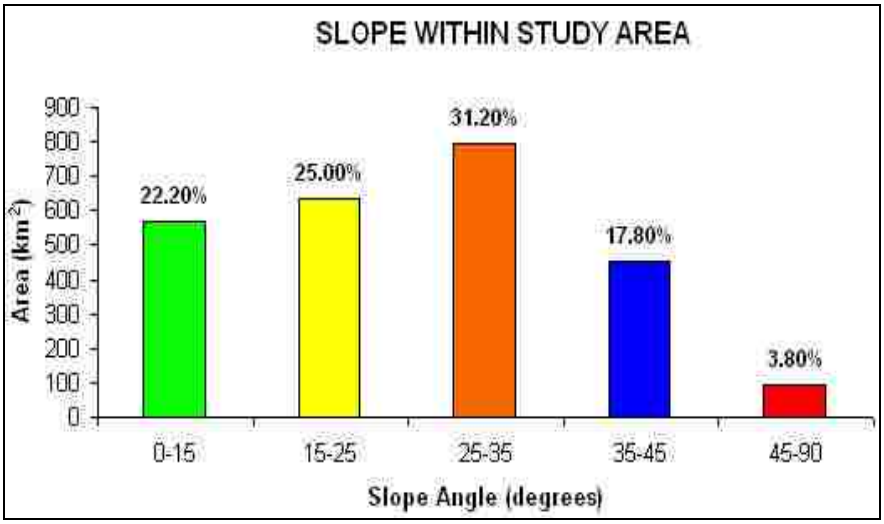

Figure 13: Bar graph indicating a percentage breakdown of slope within the study area.

6. Aspect

Slope aspect also has an influence on slope failure due to the amount of direct sunlight hitting each slope face. This in turn corresponds to the amount of snow melt and water infiltration into the slope. Also, during the winter and spring months the water infiltration is subjected to freeze-thaw cycles, breaking up packs of unconsolidated material and bedrock increasing the risk of potential mass wasting events. Within the study area, slope aspect was dispersed evenly, with the southern and eastern faces

recording only a marginally higher percentage of slope aspect (13%) than the northern and western faces (12%) (Table 4).

Table 4. Table indicating a breakdown of slope aspect within the study area.

Aspect	**Area (km^2)**	**Area (%)**
North	307	12.0
Northeast	327	12.8
East	323	12.7
Southeast	325	12.7
South	326	12.8
Southeast	328	12.9
West	299	11.7
Northwest	314	12.3
Total	**2,549**	**100**

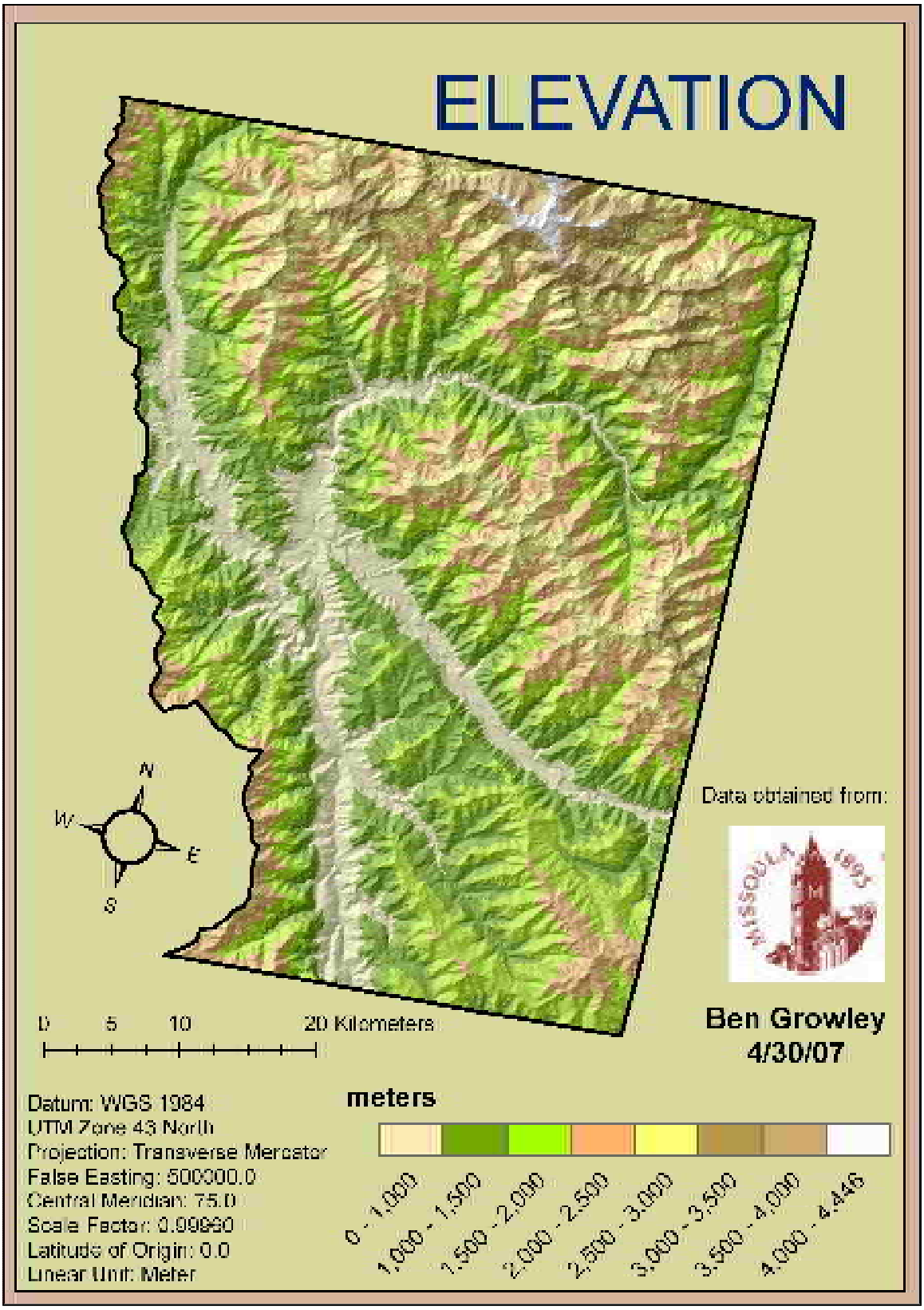

Figure 14. Elevation intervals within the study area.

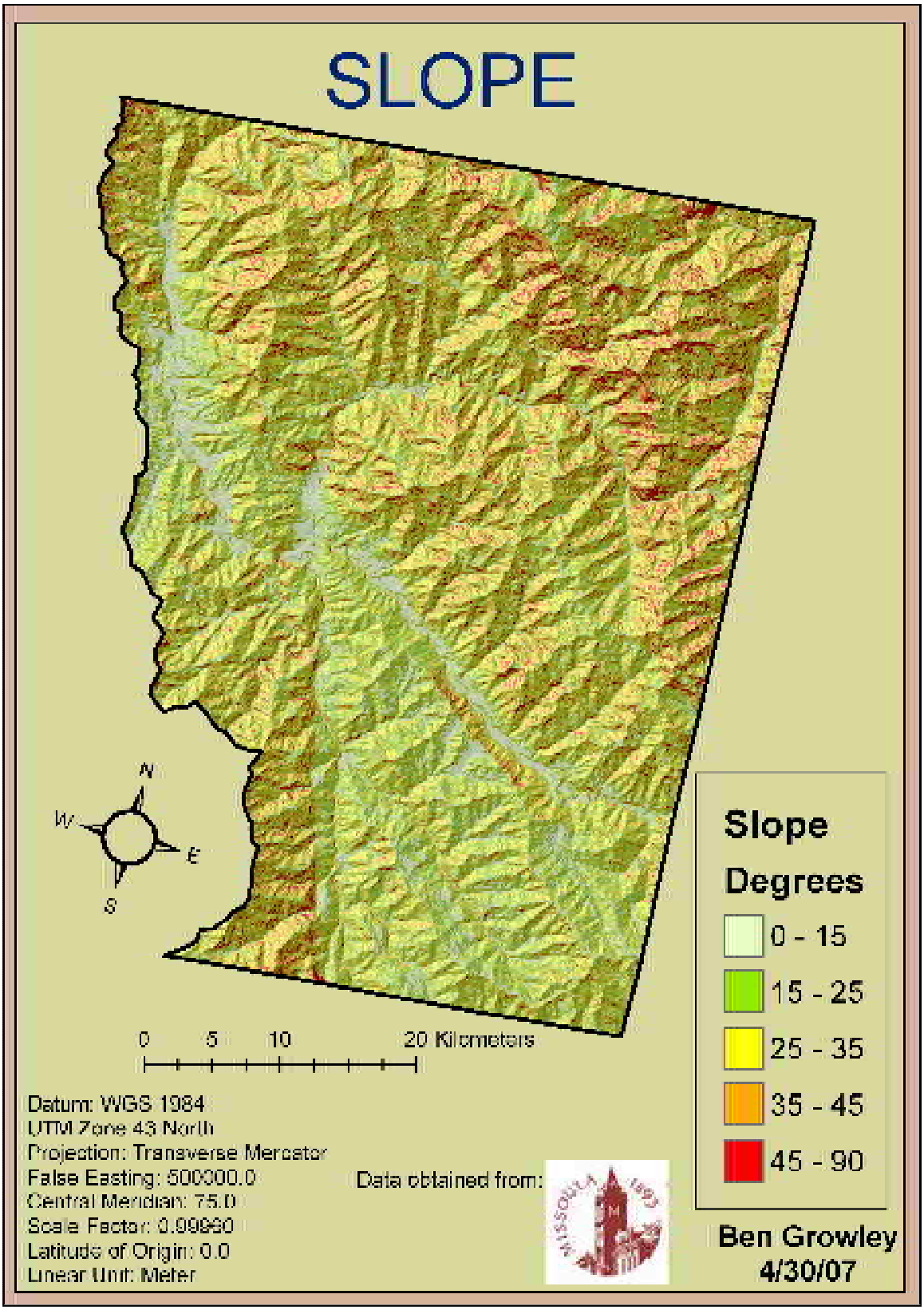

Figure 15. Slope classes within study area.

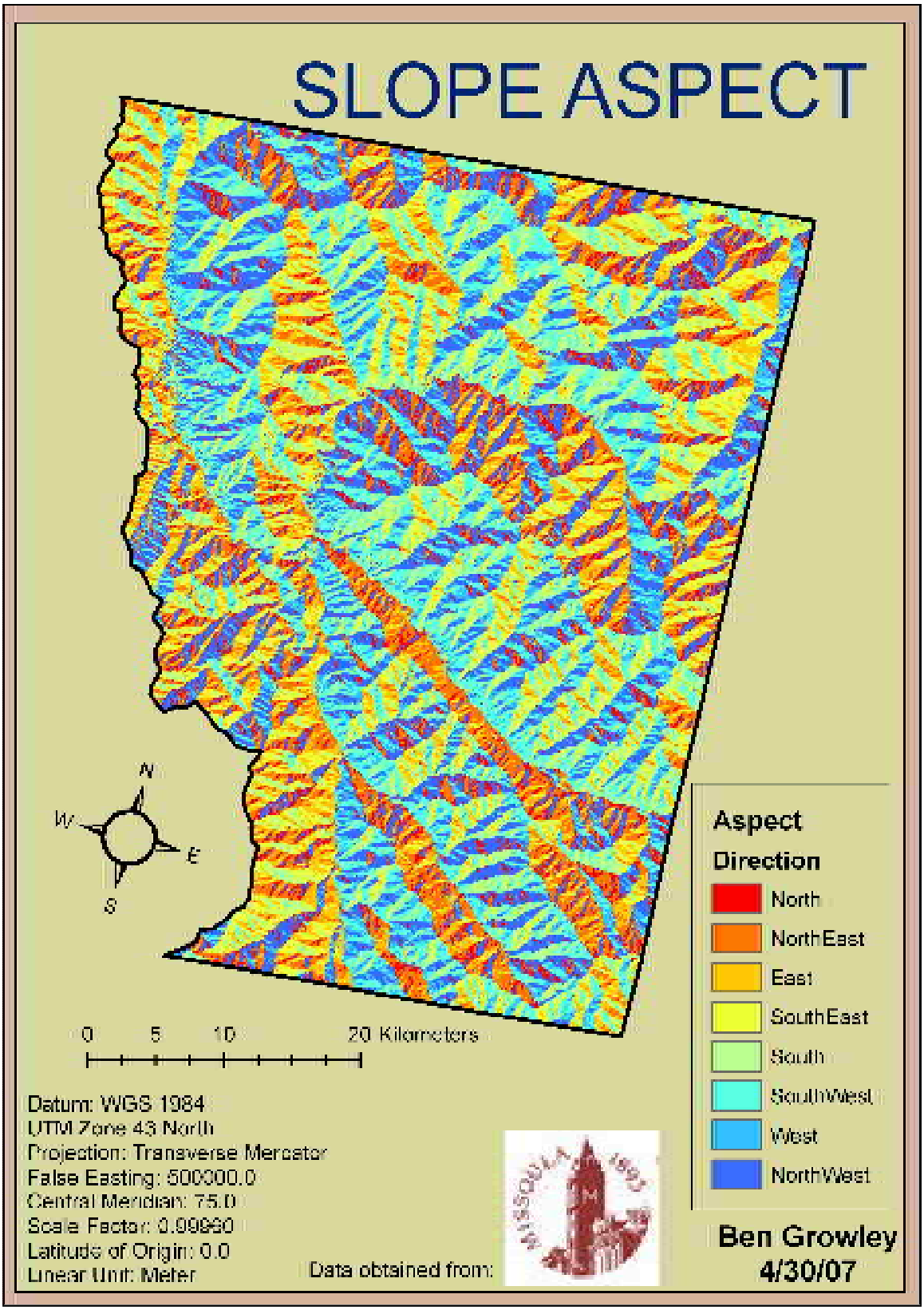

Figure 16. Slope Aspect classes within study area.

7. Roads, Rivers, and Tributaries

Attribute data for roads, rivers, and tributaries were obtained from the United Nations (U.N.) databank and covered most of study area, except a small portion of the north-western study area for the tributaries attribute, and the south-western study area west of the Jhelum River for both the road and tributaries attributes. Unfortunately, the datasets for roads and tributaries were found to be highly inaccurate when zoomed into a scale larger than 1:100,000. To correct for this inaccuracy each line segment was manually edited in ArcMap and aligned to its proper geographic location. This was difficult for roads because their spectral reflectance and the 15 m satellite imagery resolution did not allow for unambiguous identification. Digitizing tributaries was relatively easy because of the natural geomorphic paths they follow, i.e., digitizing using the ASTER imagery and DEM by following major valley arteries was possible (see Figure 20).

The rivers attribute layer consists of the Jhelum, Kunhar and Neelum rivers, which were digitized from the ASTER imagery (Figure 19). The Jhelum, Neelum and Kunhar rivers flow very rapidly with annual discharges of 11.85, 6.10, and 2.00 million acre-feet (MAF[9]), respectively, which leads to high river incision and erosion rates (Pakistan Water Gateway, 2007).

The study area contains a dense network of roadways that weave throughout the mountainous region (Figure 21). Road conditions range from paved two lane highways

[9] MAF, million acre-feet, is a unit used to describe the annual discharge of a river. One acre–foot is equivalent to the amount of water which would flood one acre to a depth of one foot (International Rivers Network, 2007).

to the more common one lane dirt or gravel lane. These roads often follow the banks of rivers, further undercutting and weakening the hill slope.

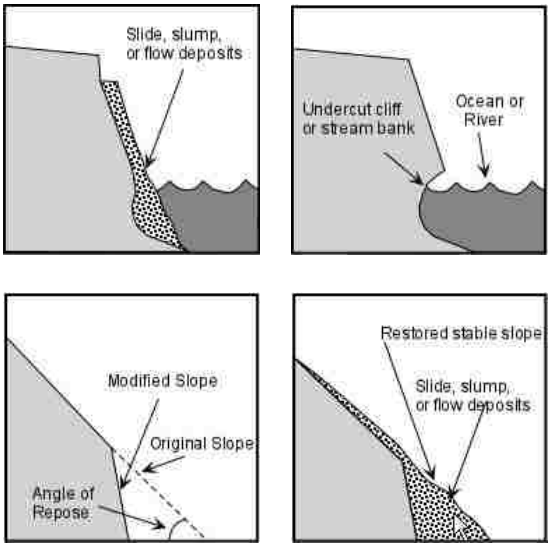

Figure 17. Effects of road and river cuts on hill slope stability (Earth Science Australia, 2007).

Modification of a slope by humans (road cuts) or natural causes (rivers and tributaries) changes the slope angle so that it is no longer at the angle of repose. This makes the slope more susceptible to mass-wasting events which can then restore the slope to its angle of repose (Figure 17). Observations in the field revealed many slope failures along road cuts and river banks. These observations suggest that the large removal of base materials by both road cuts and river incision create highly unstable slopes, which in turn may create hazardous road blocks that prevent the flow of people and resources (Figure 18).

Figure 18. Landsliding along a road that was cut into a steep slope. In many cases such landsliding caused road blockages, sometimes making them impassable for days until emergency crews could respond.

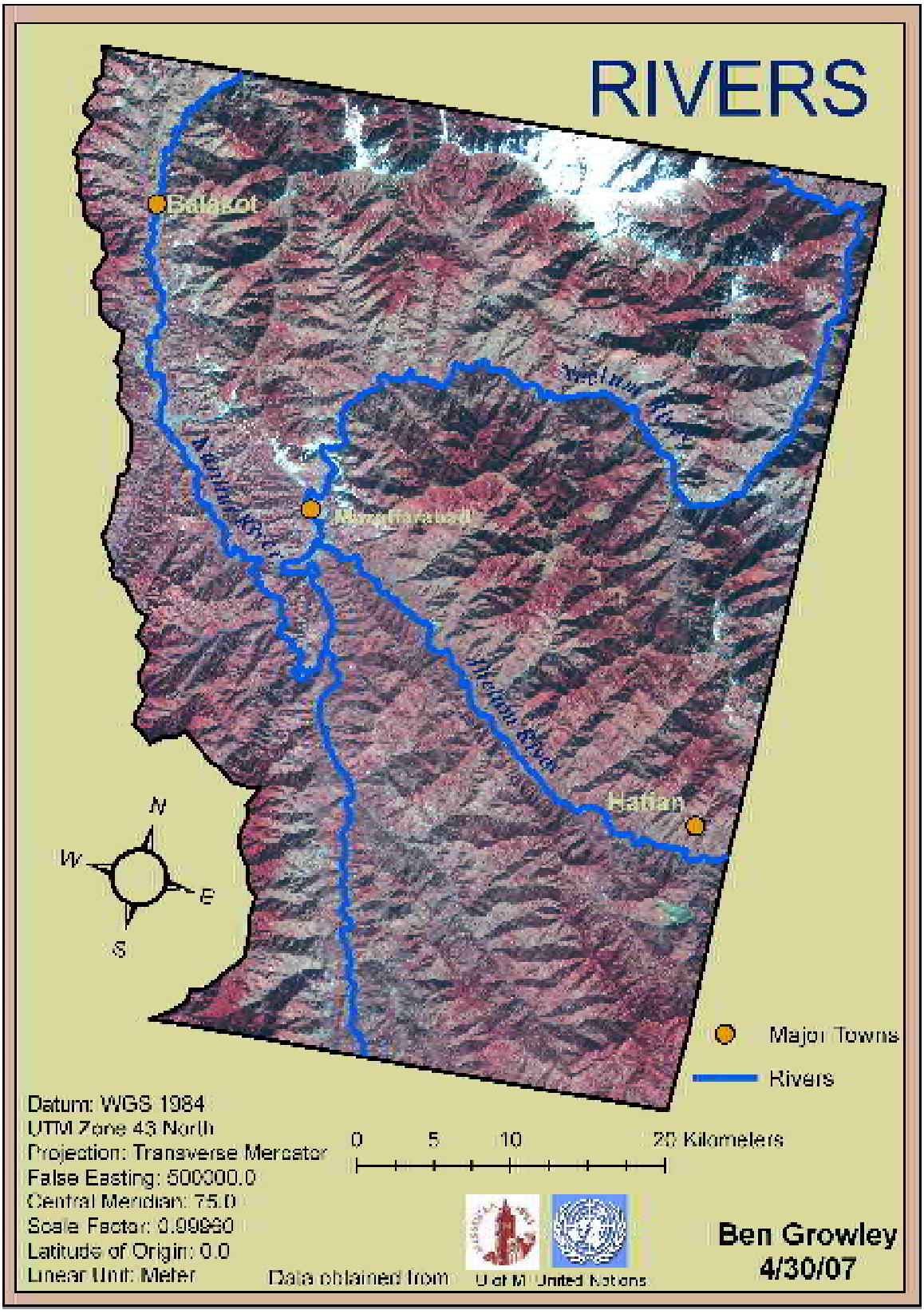

Figure 19. Rivers found within the study area.

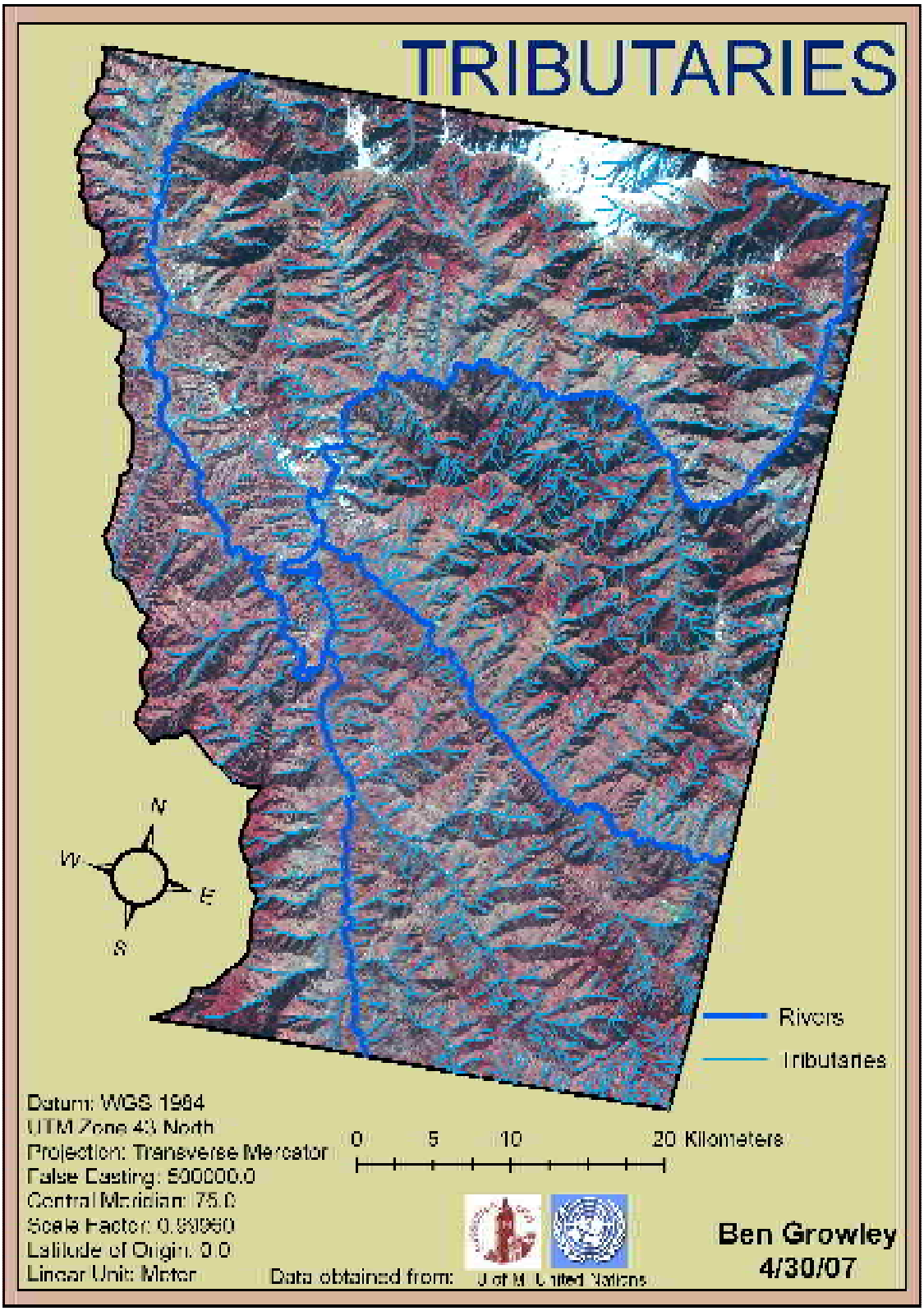

Figure 20. Tributaries found within the study area.

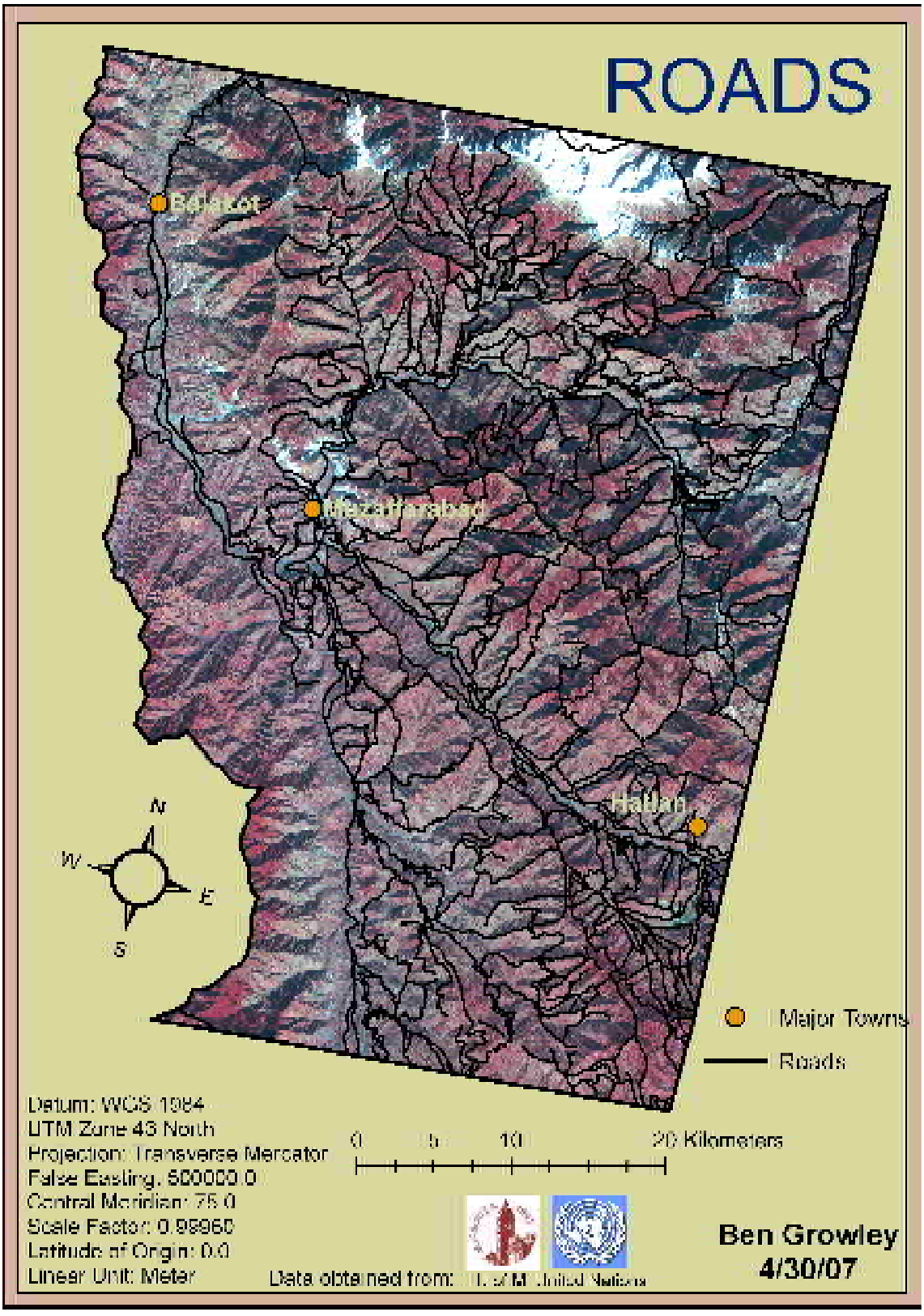

Figure 21. Roads found within the study area.

VII. PRE- AND POST-EARTHQUAKE LANDSLIDING

The results from the landslide inventories of 2005 and 2001 were analyzed against the nine attributes known to influence slope failure rates. This comparison was done for two reasons: first, to obtain data to standardize the attribute rankings for the Multi-Criteria Evaluation (MCE) and second, to compare and contrast how the different attributes affected slope failure immediately after an earthquake event and during times of relative stability. The final landslide inventory results for the post-earthquake image covered an area of 60.83 square kilometers with an average area of 0.027 km². The pre-earthquake failures combined to cover 8.33 square kilometers and an average area of 0.02 square kilometers. Approximately 371 failures in 2001 and 2,252 failures occurred in within the 2549km^2 study area.

1. Geology

The Murree formation contained the majority of failures in both the pre and post earthquake images containing 63.40% and 42.01% of the total failures respectively. The post-earthquake image shows the most impacted formation is the Kingriali with 4.26% of the formation area destroyed by failures averaging 35,904 m^2. Tanawai has the highest density of failures of any formation.

The pre-earthquake image shows the most impacted formation is the Kingriali with 3.26% of the formation area destroyed by failures. The Murree formation had the highest density of failures in the pre-earthquake image. The results show that some formations within the study area, namely Kingriali, Tanawai, Murree and Salkhala have a higher risk for slope failure. Tables 5A and B below show the results for all the landslide lithology analysis.

Tables 5A & B.
Results of the landslide inventory and the geologic attribute for the both the 2005 (A) and 2001 (B) earthquake analysis.

2001

Formation	Area (km²)	# of LS	LS Area (km²)	LS (%)	Mean LS Area (thousand m²)	LS area in formation area (%)	LS per km²
Murree	1,314	155	3.4	42.0	21.7	0.3	0.1
Hazara	284	61	1.7	16.5	28.7	0.6	0.2
Kamlial	206	19	0.3	5.2	16.9	0.2	0.1
Kingrali	74	42	0.9	11.4	20.9	1.2	0.6
Manshera	145	11	0.2	3.0	16.1	0.1	0.2
Panjal	79	15	0.2	4.1	16.5	0.3	0.2
Salkhala	348	53	1.2	14.4	21.9	0.3	0.2
Tanawai	4	5	0.1	1.4	26.2	3.3	1.3
Samana Suk	8	2	>0.0	0.5	3.2	0.1	0.3
Kawagarh	4	0	0.0	0.0	0.0	0.0	0.0
Alluvium	50	6	0.2	1.6	35.2	0.4	0.1

2005

Formation	Area (km²)	# of LS	LS Area (km²)	LS (%)	Mean LS Area (thousand m²)	LS area in formation area (%)	LS per km²
Murree	1,314	1327	30.6	63.4	23.1	2.3	1.0
Hazara	284	123	2.0	5.9	16.4	0.7	0.4
Kamlial	206	75	1.4	3.6	18.8	0.7	0.4
Kingrali	74	88	3.2	4.2	35.9	4.3	1.2
Manshera	145	66	0.7	3.2	11.0	0.5	0.5
Panjal	79	86	2.5	4.1	28.5	3.1	1.1
Salkhala	348	308	6.9	14.7	22.5	2.0	0.9
Tanawai	4	13	0.1	0.6	6.1	2.0	3.3
Samana Suk	8	0	0.0	0.0	0.0	0.0	0.0
Kawagarh	4	0	0.0	0.0	0.0	0.0	0.0
Alluvium	50	7	0.1	0.33	14.7	0.2	0.1

2. Faults

Tables 7 and 8 show the slope failure results for both pre and post-earthquake analyses. Three 100 meter buffer intervals were established around each of the fault

lines. These intervals were set up due to a "zone of destruction" 200-300 meters from the major fault lines, indicating the possible extent of their influence in slope failure (Hussain, 2006). The difference between the pre and post earthquake fault lines results was only 2.22%, which suggest that fault lines have a similar influence in mass movement regardless of an earthquake event. About 254 or 11.28 percent of all slides were accounted for in the post-earthquake 300 meter buffer analysis. The same analysis for the pre-earthquake image yielded 50 or 13.55% of all failures.

Tables 6A & B.
Results of the landslide inventory and the fault lines attribute for the both the 2001 (A) and 2005 (B) earthquake analysis.

2001

Fault Lines buffer zones	# of Slides	Percent (%)	Mean LS Area (thousand m²)	Sum Area of Slides (km²)
0-100m	26	7.1	32.8	0.9
0-200m	35	9.5	28.2	1.0
0-300m	50	13.6	31.6	1.6

2005

Fault Lines buffer zones	# of Slides	Percent (%)	Mean LS Area (thousand m²)	Sum Area of Slides (km²)
0-100m	141	6.3	70.7	10.0
0-200m	207	9.2	63.1	13.1
0-300m	254	11.3	56.1	14.3

3. Land Cover

An overwhelming majority of slope failures, about 67% in 2005 and 59% in 2001, were found to be located within the shrubs/grassland class. At approximately 20% and 18%, agricultural areas were found to be the second most susceptible land cover class; only < 3% of all failures occurred under forest cover despite being the land cover class with the most overall area covering approximately 45% of the study area. The post-

earthquake image showed that the 2.4% of the study area was devastated by landslides. In the pre-earthquake image only 0.3% is attributed to landslides; an increase of 2.1% after the 7.6 magnitude earthquake struck.

Tables 7A and B.
Results of the landslide inventory and the land cover attribute for the both the 2001 (A) and 2005 (B) earthquake analysis.

2001

Land Cover classes	Area (km^2)	Area (%)	LS Area (km^2)	LS Area (%)	LS Area in Land Cover (%)
Water	35	1.4	0.0	0.0	0.0
Urban	14	0.5	0.0	0.0	0.0
Snow/Ice	27	1.1	0.3	4.0	0.2
Forest	1148	45.0	1.4	17.0	0.1
Shrub/Grassland	1068	41.9	5.0	59.0	0.4
Agriculture	164	6.4	1.6	18.0	1.6
Unclassified	94	3.6	0.3	2.0	---
Total	2549	100	8.5	100	0.3

2005

Land Cover classes	Area (km^2)	Area (%)	LS Area (km^2)	LS Area (%)	LS Area in Land Cover (%)
Water	35	1.4	0.0	0.0	0.0
Urban	14	0.5	0.0	0.0	0.0
Snow/Ice	27	1.1	0.2	0.3	0.8
Forest	1148	45.0	1.4	2.3	0.1
Shrub/Grassland	1068	41.9	41.1	67.3	3.8
Agriculture	164	6.4	12.0	19.7	7.3
Unclassified	94	3.6	6.3	10.4	---
Total	2549	100	61.1	100	2.4

4. Elevation

Roughly 48% of the slope failures resided in the 1000-1500 meter class in the post-earthquake image and ~53% in the pre-earthquake image. The elevation attribute shows very similar results for both time frames with an average of 88.17% of all movements occurring between elevations of 500 and 2000 meters. Little to no mass wasting occurred in at an elevation above 3000 meters for either image.

Tables 8A and B.
Results of the landslide inventory and the elevation attribute for the both the 2001 (A) and 2005 (B) earthquake analysis.

2001

Elevation (m asl)	Area (km²)	Area (%)	LS Area (km^2)	LS Area (%)	LS Area in Elevation (%)
0-500	0.2	>0.0	>0.0	>0.0	0.1
500-1000	311	12.2	2.1	24.7	0.7
1000-1500	710	27.9	4.4	53.0	0.6
1500-2000	667	26.2	0.9	10.5	0.1
2000-2500	443	17.4	0.5	6.5	0.1
2500-3000	263	10.3	0.3	3.7	0.1
3000-3500	106	4.2	0.1	1.7	0.1
3500-4000	35	1.4	0.0	0.0	0.0
4000-4446	14	0.5	0.0	0.0	0.0
Total	2549	100	8.5	100.0	0.3

2005

Elevation (m asl)	Area (km²)	Area (%)	LS Area (km^2)	LS Area (%)	LS Area in Elevation (%)
0-500	0.2	>0.0	>0.0	>0.0	5.7
500-1000	311	12.2	11.5	18.9	3.7
1000-1500	710	27.9	29.3	48.0	4.1
1500-2000	667	26.2	13.0	21.2	1.9
2000-2500	443	17.4	3.6	5.8	0.8
2500-3000	263	10.3	2.4	3.9	0.9
3000-3500	106	4.2	1.3	2.1	1.2
3500-4000	35	1.4	>0.0	>0.0	>0.0
4000-4446	14	0.5	>0.0	>0.0	>0.0
Total	2549	100	61.1	100	2.4

5. Slope

Analysis of the post-earthquake slope layer shows a vast majority (~41%) of the landslide pixels fall between 25 and 35 degrees with the two flanking classes containing most of the remaining pixels (~49%) (Tables 13 and 14). The pre-earthquake image shows similar results with about 46% of landslide pixels falling in the 25-35 degree slope range and about 44% of the pixels falling in the categories falling on either side of the 25-35 degree slope category. Little landsliding occurred on slopes with angles greater than 45 degrees.

Tables 9A and B.
Results of the landslide inventory and the slope attribute for the both the 2001 (A) and 2005 (B) earthquake analysis.

2001

Slope (degrees)	Area (km²)	Area (%)	LS Area (km^2)	LS Area (%)	LS Area in Slope (%)
0-15	566	22.2	0.8	9.1	0.1
15-25	637	25.0	2.0	23.7	0.3
25-35	795	31.2	3.7	45.5	0.5
35-45	455	17.8	1.7	19.8	0.4
45-90	96	3.8	0.2	1.9	0.6
Total	2549	100	8.5	100	0.3

2005

Slope (degrees)	Area (km²)	Area (%)	LS Area (km^2)	LS Area (%)	LS Area in Slope (%)
0-15	566	22.2	4.3	7.1	0.8
15-25	637	25.0	18.1	29.7	2.8
25-35	795	31.2	25.1	41.0	3.2
35-45	455	17.8	12.7	20.7	2.8
45-90	96	3.8	0.9	1.5	0.9
Total	2549	100	61.1	100	2.4

6. Aspect

About 71% of all slope failures in the post-earthquake image fell between the southeast and southwest categories with the next highest categories falling on eastern and western slopes. A similar result for the pre-earthquake image (65%) was also shown to exist for all southern facing slopes. Northward facing slopes only accounted for between seven and eight percent of all slope failures for both time periods.

Tables 10A and B.
Results of the landslide inventory and the slope aspect attribute for the both the 2001 (A) and 2005 (B) earthquake analysis.

2001

Aspect	Area (km^2)	Area (%)	LS Area (km^2)	LS Area (%)	LS Area in Aspect (%)
North	307	12.0	>0.0	>0.0	>0.0
Northeast	327	12.8	0.4	5.3	0.1
East	323	12.7	1.6	19.4	0.4
Southeast	325	12.7	2.2	26.4	0.5
South	326	12.8	1.6	18.7	0.3
Southeast	328	12.9	1.7	19.8	0.3
West	299	11.7	0.6	6.9	0.2
Northwest	314	12.3	0.3	3.5	0.1
Total	2549	100	8.5	100.0	0.3

2005

Aspect	Area (km^2)	Area (%)	LS Area (km^2)	LS Area (%)	LS Area in Aspect (%)
North	307	12.0	0.2	0.3	0.1
Northeast	327	12.8	2.7	4.4	0.8
East	323	12.7	8.2	13.5	2.5
Southeast	325	12.7	13.1	21.5	4.0
South	326	12.8	12.3	20.1	3.8
Southwest	328	12.9	18.1	29.7	5.5
West	299	11.7	4.7	7.7	1.6
Northwest	314	12.3	1.8	2.9	0.6
Total	2549	100	61.1	100	2.4

7. Rivers, Tributaries, and Roads

Buffer zones for rivers, tributaries, and roads should be set to 50 meters (Van Westin et al., 2003). However, buffer zones in IDRISI are assigned using the COST tool, which creates Boolean buffer zones using cost distances which must be integers. These cost distances are measured as multiples of the pixel width or the resolution of the imagery (Eastman, 2003). The resolution of the ASTER imagery is 15 meters; therefore the buffer zone must be a multiple of 15. A distance of 60 meters was ultimately chosen

because of its congruency with the functionality of COST, and its relative proximity to the original distance of 50 meters obtained from the literature.

For rivers, Tables 11a and 11b show the slope failure within a distance of 25, 50 and 60 meters away from each major river. For both 2005 and 2001, approximately 6.5% of all landsliding was detected within the specified 60 meter zone. The 2005 post-earthquake image showed a slightly higher percentage of landsliding within all three buffer zones and a much higher mean and sum of failures, due to the intense weakening and fissuring of the slopes caused by the earthquake. In both images the sizes of the individual failures were on average larger within the smaller buffer zones indicating that the influence rivers has on slope failures diminishes with distance. Overall failures within the 60 meter buffer zone increased by 10.5 square kilometers or 1500 percent.

Tributaries showed similar results for both images, however the tributaries attribute covers a much larger area, due to the numerous mountain streams funneling into the major rivers. This is evident when viewing the number of slides as the tributaries shows about four times the amount of slope failure events than the rivers attribute (Tables 12a and 12b). However the larger more powerful flowing rivers indicate an average landslide area two to three times larger than those occurring within the buffer zone of tributaries alone.

Tables 11A and B.
Results of the landslide inventory and the rivers attribute for the both the 2001 (A) and 2005 (B) earthquake analysis.

2001

Buffer Zone (m)	Slides (#)	Slides (%)	Mean Area of Slides (thousands m²)	Sum Area of Slides (km²)
25	11	2.98	42,9	0.5
50	22	5.96	32,9	0.7
60	23	6.23	31,9	0.7

2005

Buffer Zone (m)	Slides (#)	Slides (%)	Mean Area of Slides (thousands m²)	Sum Area of Slides (km²)
25	107	4.70	87,0	9.3
50	154	6.76	69,6	10.7
60	163	7.24	68,8	11.2

Tables 12A and B.
Results of the landslide inventory and the tributaries attribute for the both the 2001 (A) and 2005 (B) earthquake analysis.

2001

Buffer Zone (m)	Slides (#)	Slides (%)	Mean Area of Slides (thousands m²)	Sum Area of Slides (km²)
0-25	88	23.9	19,7	1.7
0-50	122	33.1	20,2	2.5
0-60	130	35.2	19,8	2.6

2005

Buffer Zone (m)	Slides (#)	Slides (%)	Mean Area of Slides (thousands m²)	Sum Area of Slides (km²)
0-25	562	25.0	46,8	26.3
0-50	655	29.1	44,2	29.0
0-60	689	30.6	43,2	29.8

Road cuts in Azad Kashmir and most other parts of northern Pakistan are often created adjacent to major river conduits. Tables 13a and 13b show the 25 meter buffer zone of the rivers attribute showing a larger mean area than the 50 and 60 meter buffers. These results suggest that the influence of road cuts on the stability of a slope is greater when in close proximity to the road.

Tables 13A and B.
Results of the landslide inventory and the roads attribute for the both the 2001 (A) and 2005 (B) earthquake analysis.

2001

Buffer Zone (m)	Slides (#)	Slides (%)	Mean Area of Slides (thousands m²)	Sum Area of Slides (km²)
0-25	79	21.4	26,9	2.1
0-50	102	27.6	26,0	2.7
0-60	105	28.5	25,7	2.7

2005

Buffer Zone (m)	Slides (#)	Slides (%)	Mean Area of Slides (thousands m²)	Sum Area of Slides (km²)
0-25	478	21.2	55,5	26.5
0-50	582	25.8	48,6	28.3
0-60	618	27.4	46,7	28.9

Immediately after the earthquake new road cuts were carved into the slopes to create a path for mitigation purposes and to create new supply and transportation routes. Based on field observations and past experiences we can expect that the spring melt water will increases the volume and flow of rivers and tributaries, intensifying the undercutting process along all major rivers and tributaries

VIII. MULTI-CRITERIA EVALUATION (MCE)

Every day we make many decisions ranging from simple choices to complex assessments that require careful consideration of multiple factors. "Decision making itself is defined as a selection of alternatives and is used in many fields in both the social and natural sciences, including GIS" (Elliot, 2004 pp.5). Multi-Criteria Evaluation (MCE) is a decision support tool within the realm of GIS. The decision is a choice between alternatives or identifying priorities (landslide susceptibility). This particular study focuses on the latter and evaluates a set of factors (i.e. slope, land cover etc.) in order to generate criterion[10]. MCE merely combines these criteria to construct a single composite of which to base decision(s) according to a specific objective[11]. The stated objective for this MCE is to assess the designated study area to determine landslide susceptibility.

There are a number of various methods used in MCE, some of them qualitative in nature such as the Analytical hierarchy process (AHP) (Saaty, 1980) and weighted linear combination (WLC). Other methods are purely statistical in nature such as Bivariate statistical analyses (BSA) and the multivariate statistical approach (MSA) (Ayalew, 2005). This study will make use of the AHP method because of its precision, ease of use and because it's an integrated methodology within the software used to carry out the analysis.

[10] Criterion is considered a generic term that includes both the concepts of attribute and objective. (Malczewski, 1999).
[11] "An objective is a statement about the desired state of the system under consideration which relates to, or is derived from a set of attributes." (Malczewski, 1999).

The analytical hierarchy process was developed by Thomas Saaty (1980) and is one of the most GIS-friendly methods available. It is a built in component of IDRISI (Andes version). Weights for each criterion are determined by a pair-wise comparison using a ratio matrix. The pair-wise comparison will be discussed later in detail.

All nine attribute layers with the exception of land cover were developed and prepared using ESRI's ArcMap 9.2 and ArcCatalog 9.2. The land cover attribute map was created using IDRISI and then exported into ArcMap. Once all the layers were spatially correct, they were then exported as either shapefiles or ASCII files, because of IDRISI's ability to import those particular formats. The next step in the process would be to standardize the scale of each attribute included in the MCE model, however before that work can commence; statistics were gathered on the various attributes influence or susceptibility to mass movement within the study area. For instance, which of the formations within the geological attribute layer is most vulnerable to mass movement? To obtain these statistics, a landslide inventory map was produced using ESRI's feature analyst extension, for both pre- and post earthquake images as shown in Chapter 7.

The first step in the MCE protocol was configuring the weights of the attributes and assigning the amount of influence each attribute has on the final susceptibility map. A pair-wise analysis developed by Thomas Saaty (1990) was used to accomplish this task. This approach employs an underlying scale (Table 14) with values from 1 to 9 to rate the relative preference on a 1:1 basis of each criteria (Malczewski, 1999). The rationalization behind choosing the values was based on previous landslide susceptibility and hazard mapping studies and expertise gained from the field campaign.

Table 14. Pair-wise comparison rating scale with nine divisions.

Intensity of Importance	Definition	Explanation
1	Equal importance	Contribution to objective is equal
3	Moderate importance	One attribute slightly favorable over another
5	Strong importance	Attribute strongly favored over another
7	Very strong importance	Attribute is favored very strongly over another
9	Extreme importance	Evidence favoring one attribute is of the highest possible order of affirmation
2,4,6,8	Intermediate values	When compromise is needed

Taking hard quantitative values and assigning them linguistic expressions that translate into an imprecise terminology creates a vast area of ambiguity concerning the results. However, "the linguistic expressions explain the fact that the state of knowledge is imperfect; while the numerical values are quantified translations useful for calculating factor weights. Science still lacks a direct way of evaluating intuition or expressions, and the validity of the numerical values may best be judged by the factor weights and the consistency of the calculation process" (Ayalew, 2004 pp 79).

Table 15. Pair-wise matrix showing calculated factor weights for all nine attributes.

Pair-Wise	Aspect	Elevation	Faults	Geology	Land Cover	Rivers	Roads	Slope	Tributaries
Aspect	1								
Elevation	2	1							
Faults	6	5	1						
Geology	7	6	3	1					
Land Cover	4	4	1/3	1/5	1				
Rivers	4	4	1/3	1/5	1	1			
Roads	4	4	1/3	1/5	1	1	1		
Slope	7	5	2	1	4	4	4	1	
Tributaries	1/3	1/4	1/7	1/8	1/6	1/6	1/6	1/8	1

Table 16. Scaled weight of each attribute used in the final landslide susceptibility calculation.

Factor	Weight
Aspect	0.0267
Elevation	0.0358
Fault Lines	0.1607
Geology	0.2840
Land Cover	0.0790
Rivers	0.0790
Roads	0.0790
Slope	0.2389
Tributaries	0.0169

The result of the pair-wise comparison seen in Table 16 is the generation of scaled weight for each attribute which were then were calculated into the final MCE.

Geology was identified as the most heavily weighted factor at 0.28, followed by Slope at 0.23 and Faults at 0.16. Aspect, Elevation and Tributaries were the least contributing attributes with each only accounting for about 8% of the total weight. Land cover, Rivers, and Roads held equal weight assuming equal importance in the final map.

The consistency ratio (CR) indicates the probability that the matrix rating was randomly generated and ranges in scale from 0-1. Saaty (1990) recommended a CR <0.10; the CR in this study was found to be 0.05

IX. LANDSLIDE SUSCEPTIBILITY

Now that the landslide inventories have been completed, and all attributes successfully scaled and weighted the final susceptibility zonation maps can be produced. The final susceptibility maps, created in IDRISI, were exported into ArcMap 9.2 for data analysis and thematic breakdown of risk levels. First, the image was clipped to conform to the boundaries of the study area; then, the 0-255 susceptibility scale was broken into four easily read and understandable risk levels and assigned an appropriate corresponding color.

1. Susceptibility Success Rate

A success rate curve was used to accomplish these tasks and is a common technique used in susceptibility mapping (Neuhauser, 2006; Lee, 2004; Van Westin, 2001; Zezere, 2004). The susceptibility analysis results were verified using the known landslide locations from the landslide inventory map compared with the landslide susceptibility map. This generated a success rate curve that illustrated how well the susceptibility maps for 2001 and 2005 predict landslides and created a visual presentation of the suitability of the assessment. The area under the curve allows for an evaluation of the prediction's accuracy with 1 indicating 100% prediction accuracy. Landslide susceptibility mapping accuracies according to success rate curves vary widely from study to study with results ranging from 61.9% to 93.2% (Lee, 2006; Vijith, 2007; Dahal, 2008). In this study, the accuracy of the 2005 susceptibility map (Figure 22 B) is 67% and thus, is acceptable. For the 2001 susceptibility map (Figure 22 A) the accuracy is

only 50% which puts the results in question. This may be due in part to the relative small number and size of the individual landslide inventory training sites.

Figure 22. (A) 2001; (B) 2005. Landslide Susceptibility Curves

2. Susceptibility Classes

To obtain the boundaries for each risk level, the calculated index values of all cells in the susceptibility map were sorted in descending order. An excel sheet was constructed to hold these values along with the number of landslide pixels and associated area percentage for every classification value (0-245). This list was used to determine where each class break would occur in each susceptibility map. The final map values were then classified using the maps derived success rate curve. Four susceptibility levels were identified in this susceptibility mapping, ,with each level assigned a linguistic expression of low, moderate, high, or very high and colors of green, yellow, orange, and red (Ramakrishnan, 2002; Roa, 2007) (Tables 17 A and B). Thresholds for the "very high" and "high" class were given a higher interval range in the classification breakdown since they are often underestimated. This means that areas in the "very high" class have a landslide susceptibility probability of >70%.

Table 17 (A) 2001; (B) 2005. Thresholds at which individual pixels were assigned their susceptibility class.

2001 Threshold Risk Level Breaks		
Cumulative landslide occurrence to be predicted (%)	Threshold at index value	Assigned susceptibility class
[0 – 20]	up to77	LOW
[20 – 40]	up to 85	MODERATE
[40 – 70]	up to 100	HIGH
[70 – 100]	over 100	VERY HIGH

2005 Threshold Risk Level Breaks		
Cumulative landslide occurrence to be predicted (%)	Threshold at index value	Assigned susceptibility class
[0 – 20]	up to 105	LOW
[20 – 40]	up to 120	MODERATE
[40 – 70]	up to 137	HIGH
[70 – 100]	over 137	VERY HIGH

3. Susceptibility Maps

The final susceptibility maps were produced at a scale of 1:400,000 (Figures 23 and 24). The amount of area that falls into each susceptibility class differs greatly from 2001 to 2005 (Tables 17 A and B). The greatest change from 2001 to 2005 occurred in the "very high" (-15.9%) and "low" (+18.7%) classes. The "moderate" (+3.2%) and "high" (-6.0%) classes fluctuated little between both years. The overall trend was a large shift (~558 $km^{2)}$ of "high" and "very high" susceptibility in 2001 to "moderate" and "low" susceptibility in 2005.

Tables 18 (A) 2001; (B) 2005. Amount of study area contained within each susceptibility class.

SUSCEPTIBILITY MAP 2001		
Susceptibility Class	**Area (km^2)**	**Area (%)**
Low	492	19.3
Moderate	656	25.7
High	731	28.7
Very High	670	26.3
Total	2549	100

SUSCEPTIBILITY MAP 2005		
Susceptibility Class	**Area (km^2)**	**Area (%)**
Low	969	38.0
Moderate	737	28.9
High	577	22.7
Very High	266	10.4
Total	2549	100

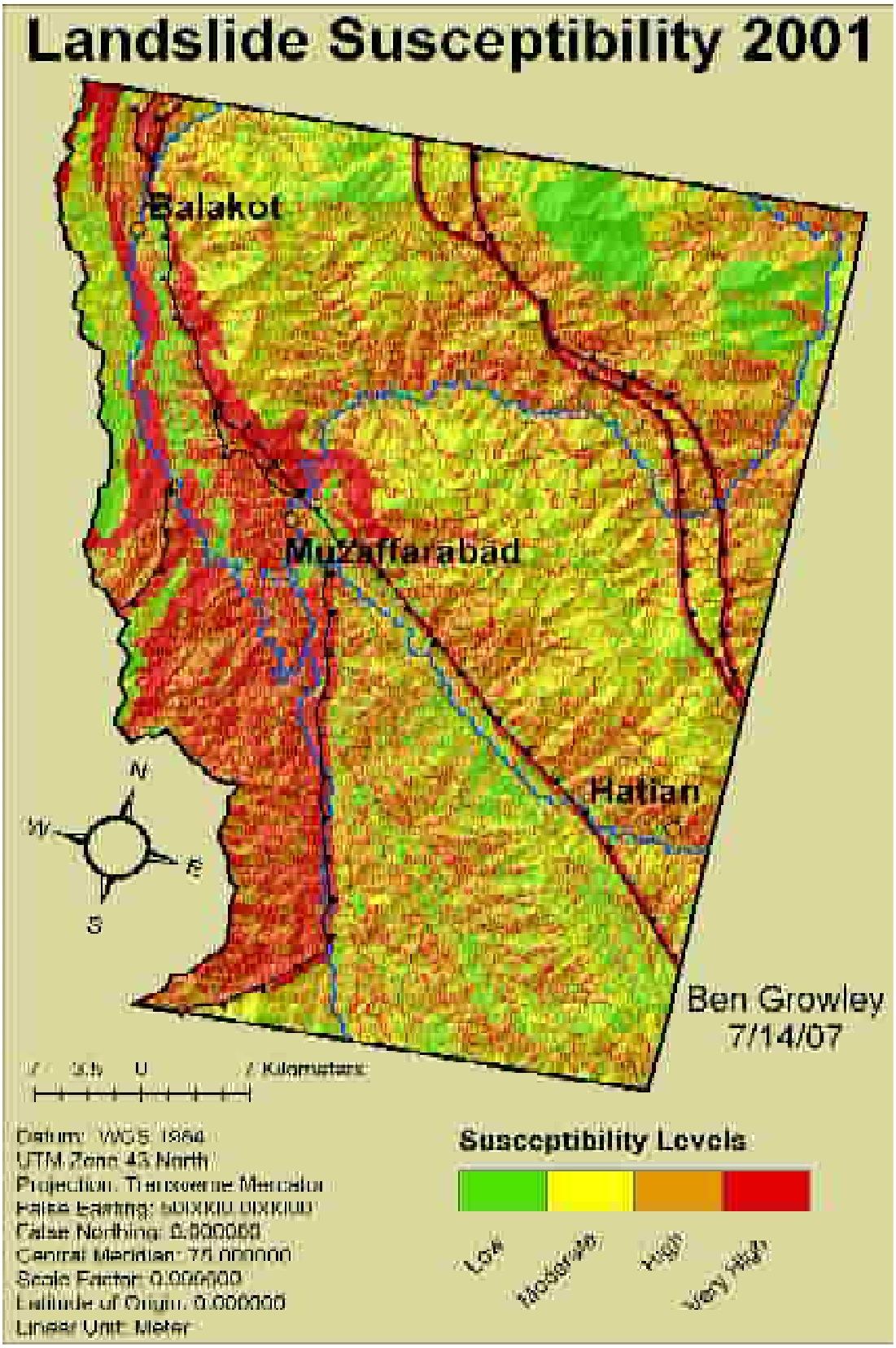

Figure 23 Final Susceptibility map for 2001.

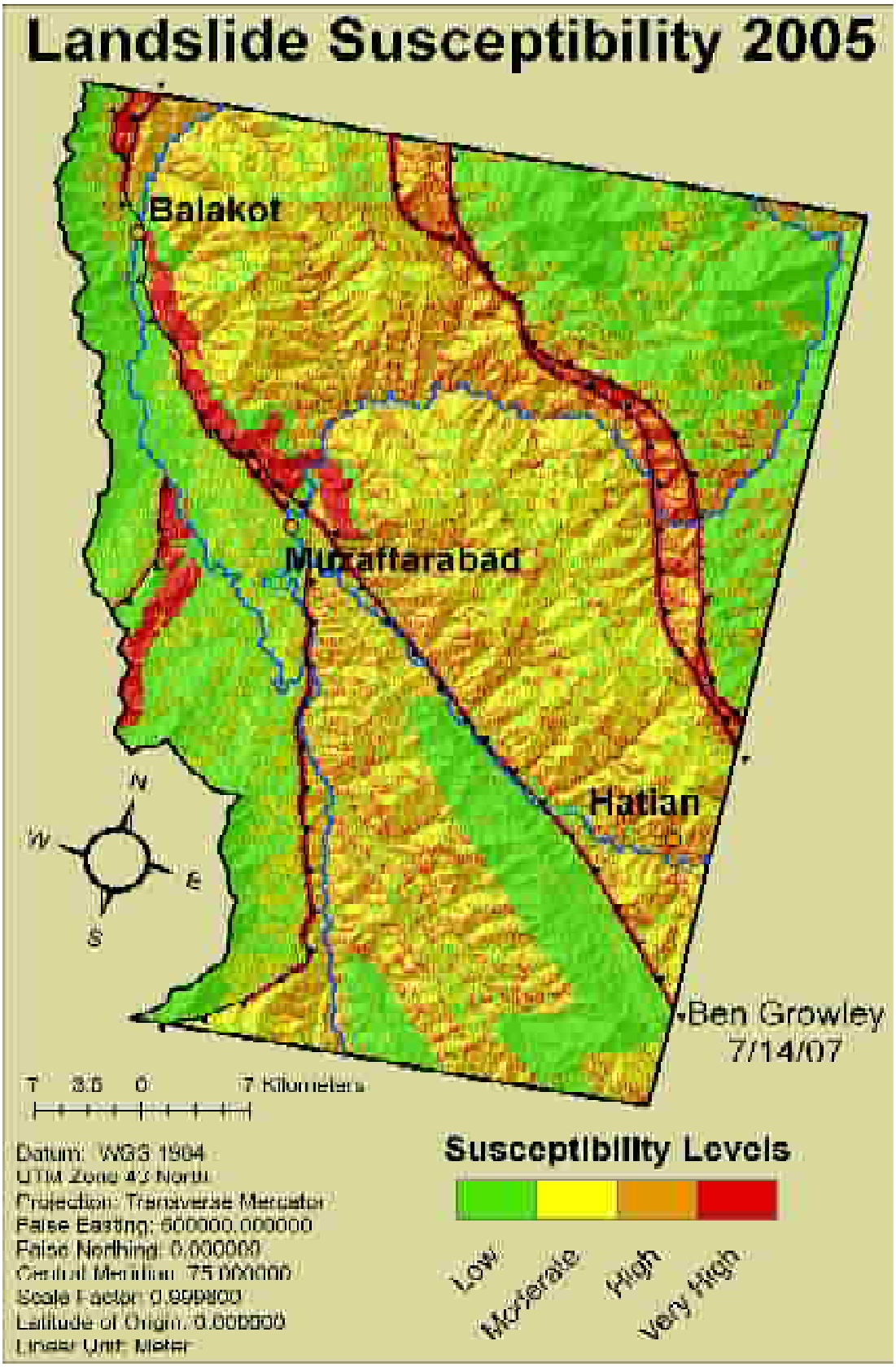

Figure 24 Final Susceptibility map for 2005.

In 2001, all four susceptibility classes are evenly represented, while 2005 shows about 67% of the study area was classified as being of either "low" or "moderate" susceptibility to future landsliding (Table 18 B). Both maps underline the strong impact of the geological formations on landsliding; thus, supporting the results from many other studies (Brabb, 1984). A majority of the area within the Murree and Hazara formations falls into the "moderate" and "high" susceptibility classes. These two formations contain shale and slate, respectively, which are relatively weak rocks. In general, the results from the susceptibility mapping match the outlines of several formations. For instance, both susceptibility maps delineate the Manshera Formation in the north-east portion of the study area: its granitic composition commands a low level of susceptibility. In the same manner, the Kingriali and Tanawai formations are both categorized in the "very high" susceptibility classes. One key difference concerning geology is the "low" susceptibility outline of the Kamlial Formation in the south-east portion of the 2005 map, which is not present in the 2001 map. This phenomenon is not a result of the influence of the lithology but rather the large decrease in the importance of the surrounding Murree Formation from 2001 to 2005. In addition to geologic formations and slope, areas adjacent fault lines are of high susceptibility.

The city of Muzaffarabad is settled on a large flat area of land, thus, is characterized by "low" susceptibility to landsliding in the 2005 map. However, the surrounding area of Muzaffarabad partly lies adjacent to the Kingriali Formation and the Balakot-Bagh fault; thus, it is part of the "high" susceptibility class. This surrounding is densely populated and many people commute to and from the city on a daily basis. The

2001 map places patches of every risk level around Muzaffarabad, most likely due surrounding geology, presence of major rivers and faults and the dramatic changes in relief.

Balakot, a smaller city northwest of Muzaffarabad, was completely devastated by the earthquake. The 2001 map presents a moderately susceptible city area that is surrounded by areas of high and very high susceptibility. In the 2005 map, the city area is characterized by only low susceptibility; the city, however, is adjacent to an area of very high susceptibility.

Hattian is the smallest of the three urban areas portrayed on the map and is also the closest in proximity to the largest mass movement in the study area. Both 2001 and 2005 maps place Hattian surrounded by very high susceptibility levels. In addition, the city is surrounded by areas of high susceptibility.

4. Landslide Inventories versus Landslide Susceptibility

In addition to the success rate curves generated to evaluated the susceptibility results, for both years 2001 and 2005 the landslide inventory maps were laid over the susceptibility maps to acquire how many slope failures fall into each of the susceptibility classes. This approach produced three different scenarios: (i) 2001 landslide inventory map versus 2001 susceptibility map; (ii) 2005 landslide inventory map versus 2005 susceptibility map; (iii) 2005 landslide inventory map versus 2001 susceptibility map. Scenarios (i) and (ii) generated very similar results with about 13% of failures falling in the "low" susceptibility class, ~26% in the "moderate" susceptibility class, ~37% in the

"high" susceptibility class, and ~24% in the "very high" susceptibility class (Tables 19 and 20).

The 2005 susceptibility map shows a much higher percentage of the study area in the low susceptibility class (38.9%) compared to the 2001 map (19.3%), yet, landslide occurrence within this class remained relatively constant at ~13%. This may indicate that the 2005 map represents a more refined risk level assessment, or predicting power. This result is at least partially due to the superior landslide inventory from which the 2005 susceptibility map was created.

Table 19 Scenario i 2001 landslide inventory overlaid on the 2001 Susceptibility map.

2001 LS Inventory vs. 2001 Map			
Susceptibility Class	**Landslide Pixels (#)**	**LS Area (km^2)**	**Landslides (%)**
Low	4886	1.1	13.3
Moderate	9837	2.2	26.7
High	13870	3.1	37.7
Very High	8250	1.9	22.4
Totals	36843	8.3	100

Table 20 Scenario ii 2005 landslide inventory overlaid on the 2005 Susceptibility map.

2005 LS Inventory vs. 2005 Map			
Susceptibility Class	**Landslide Pixels (#)**	**LS Area (km^2)**	**Landslides (%)**
Low	34223	7.7	12.7
Moderate	68899	15.5	25.5
High	97175	21.9	36.0
Very High	69936	15.7	25.9
Totals	270233	60.8	100

Scenario (iii) represents an evaluation of the predicted landslide susceptibility in the 2001 map, since actual slope failures in the 2005 inventory map were compared against the 2001 susceptibility map. As shown in Table 21, ~75% of all 2005 landslides

occurred in the "high" or "very high" susceptibility classes of the 2001 susceptibility map. This high percentage translates into a high prediction success rate for the 2001 susceptibility map. Therefore, it is assumed that the 2005 susceptibility map is of similar quality for the prediction of future landsliding.

Table 21. Scenario iii 2005 landslide inventory overlaid on the 2001 Susceptibility map.

2005 LS Inventory vs. 2001 Map			
Susceptibility Class	**Landslide Pixels (#)**	**LS Area (km^2)**	**LS (%)**
Low	19053	4.3	7.1
Moderate	49884	11.2	18.5
High	130688	29.4	48.4
Very High	70608	15.9	26.1
Totals	270233	60.8	100

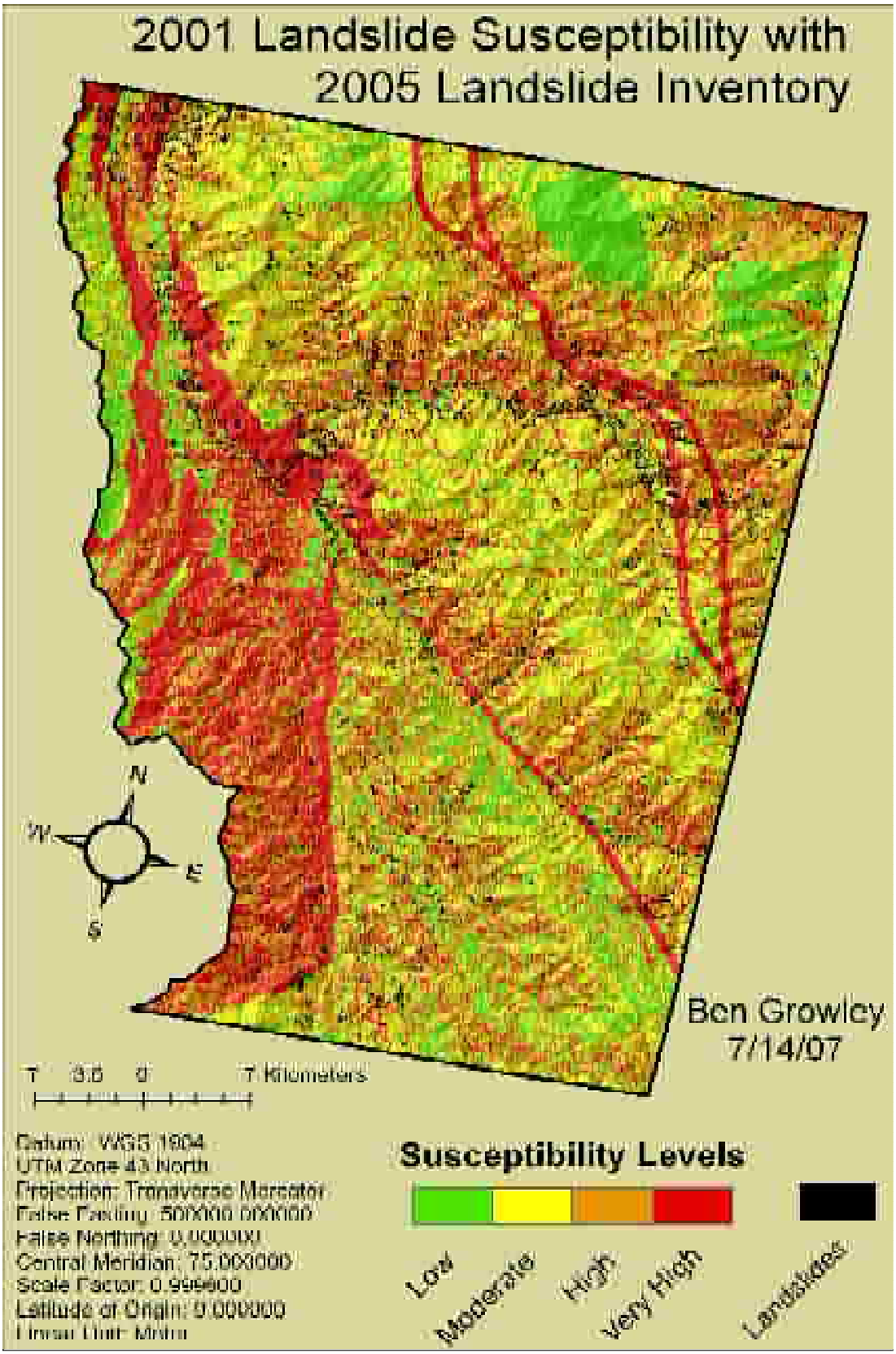

Figure 25 Map showing the 2005 landslide inventory overlaid on top of the 2001 susceptibility map.

The produced results illustrate several important trends. First, they show that the rates at which landsliding occurs within the individual attributes went largely unaffected by the cataclysmic event of October 8, 2005. Rates of 2005 post-earthquake failure varied only slightly from the pre-earthquake failure background rates in 2001 (Table 22). For example, 28.5% (105) of all landslides occurred within a 60 meter buffer of all major roads in 2001. In 2005 27.4% (618) of all landslides occurred within this same buffer. The earthquake caused the number of individual slides to increase but they were occurring at about the same rate. The average differences between failure rates for 2001 and for 2005 for each attribute are generally very low.

Table 22. Average difference in landslide occurrence rates for each attribute between the 2001 and 2005.

Attribute	Avg. Difference (%)
Roads (60m)	1.0
Rivers (60m)	1.0
Tributaries (60m)	4.6
Faults (300m)	2.3
Geology	4.0
Slope	2.8
Aspect	3.1
Elevation	2.5
Land Cover	5.2

For some attributes, however, interesting changes are noticeable. For example, in the Murree Formation failures related to slope increased from 42% in 2001to 63% in 2005, while in the Hazara Formation they decrease from 17% to 6%. Within the land cover attribute, the shrub land/grassland class absorbed most of the failures, while in forested areas, failures dropped from 17% in 2001 to 2% in 2005.

X. POST-SNOWMELT LANDSLIDING; REPEAT PHOTOGRAPHY

The susceptibility analysis evaluated the study area from ASTER imagery taken in November, 2005 approximately one month after the earthquake struck. During the ensuing six months these already weakened hill slopes are subject to the winter freeze and spring thaw, both of which can further weaken the hill sides. Field research was undertaken in that region six months after the earthquake to perform a repeat photography analysis.

Before leaving for the field, two bound books were created that contained every picture that was taken in the first field study (Owen et al, 2007). Accompanying each photograph was the GPS coordinates and the angle at which the picture was taken. This provided the researchers with a visual to compare against the scenes they would see in the field. The locations were accessed by jeep and foot and the proper angle was found using a compass set at a 2½ degree declination. All information gathered from the sites was recorded in a field book and includes GPS coordinates, GPS location number and picture number and any other relevant information that may prove useful later in the research, such as, contact zones, areas of extensive fissuring etc. The following will first explicate the results of the repeat photography and then illustrate several examples of increased slope failure.

The repeat photography method examined 258 photo pairs gathered from 138 locations. Most of these locations were located along major roadways as access to a large portion of the study area was inaccessible or extremely difficult to access. There is no way to separate the mass movements that were a direct effect of the October 8, 2005

quake. However, the purpose is not to generate a number of earthquake caused landslides, but develop multi-temporal data on additional mass movements caused by freezing temperatures and spring thaw of the winter and spring months. A total of 1,329 mass movements were recorded for the photos taken one month after the earthquake in November of 2005. The 2005 photos used in this study were taken during the field campaign of Owen et al. (2007) but are not the same photos used in that paper's analysis, so a direct comparison of the two studies is not possible. The photos from May/June 2006 revealed 1,484 slides an increase of 155 additional slides. Of the 258 photos examined, approximately 29% (75) showed either additional slides or slides that had reactivated within the six month time span. About 78% or 202 pictures in the analysis had two or more landslides in the photograph with the max found in any single scene being 30. The average number of mass movements detected in any single photograph jumped from 5.15 in 2005 to 5.75 in 2006. The following are a few examples of the findings during the repeat photography analysis. The first example (shown in Pictures 1A and B) is an area located directly above a road where seismic activity was the probable initial cause of major fissures and a slight translational slide. This situation created a potentially dangerous situation for travelers and knocked a building from its foundation directly below the road. After the spring thaw, water infiltrated these fissures and caused a large translational slide blocking the road and reeking havoc on additional structures below.

Picture 1A Site 205, 2005

Picture 1B Site 205, 2006

Pictures 2 A and B demonstrate a similar scenario as fissures on the hill side warn of an impending road block. This type of scenario is all too common and particularly

treacherous; as much of Northern Pakistan's mountainous narrow roadways weave in and out of steep slopes creating dangerous blind curves.

Picture 2A Site 140, 2005.

Picture 2B Site 140, 2006.

Picture 3A Site 095, 2005.

Picture 3B Site 095, 2006.

This is yet another example of a slope failure (Pictures 3A and B) presaged by extensive fissuring. It is important to note how after the section of road was destroyed, it was simply re-cut deeper into the cliff without any preventative measures or support structures put into place. This action only further destabilizes the slope and makes it more susceptible for future reactivation.

The next example is of a large debris fall shown in Pictures 4A and B. This type of failure is common and many times includes farmland and human settlements. The slope failure appears to be shallow, but covers a very large area which can block roads, destroy power lines, and dam rivers. Pictures 5A and B depict a reactivated failure positioned above a major river which completely stripped one aspect of the hillside. This is yet another example of how rivers can destabilize a slope by the removal of base

material. This is a low elevation slope failure which again was a very common sight when traveling along major roadways (adjacent to rivers) in the area.

Picture 4A Site 038, 2005.

Picture 4B Site 038, 2006.

Picture 5A Site 183, 2005.

Picture 5B Site 183, 2006.

Picture 6. Multiple mass movements destroying a farmer's agricultural terraces.

Figure 25 shows a photo taken in June, 2006 and exemplifies the effects mass movement can have on the people. The orange circle shows the location of a farm house with the light blue circles showing slope failures that have destroyed areas used for farming. Areas of flat land are a rare commodity in the steep landscape forcing locals to practice what is known as steep farming. With areas of the slope failing, structures and farmland are in danger of being partial damaged or completely destroyed. This photo illustrates how mass movement can have a severely negative effect on the culture and lively hood of the local people.

XII. CONCLUSION

This study utilized GIS and remote sensing technology, combined with field techniques to assess landslide activity for the 2005 Kashmir earthquake region. The collection of the slope failure data led to the creation of a GIS Landslide Susceptibility Zonation map, which can now be utilized for future hazard and risk assessment, planning and mitigation. This study contributes landslide data in an area highly prone to landslide and earthquake activity. This thesis shows that landslide controlling elements can be researched and established geospatially to better understand and predict landslide occurrence.

The study revealed that a strong relationship exits between the environmental setting of a location (attributes) and landsliding activity in the event of an earthquake. For instance, 67% of the landsliding occurred in shrub land/grassland; 48% occurred between elevations of 1000-1500 m asl; 41% occurred on slopes between 25 and 35 degrees; and over 70% occurred on slopes that had a southern exposure. These areas, therefore, can be associated with a higher susceptibility for future slope failure.

These ascertained localized settings are associated with higher susceptibility levels, which is most evident in the 2005 susceptibility map. For instance, the map demonstrates how influential the local geology is in predicting slope failure. Areas comprising the Kingriali and Panjal formations, which have the highest landslide density within formation, were almost exclusively classified as having a very high susceptibility level. Similar conclusions can be inferred from the map concerning other attribute's characteristics including, but not limited to slope, roads, and fault lines.

Rates at which landsliding occurs within each attribute remained remarkably similar in both the 2001 and 2005 analysis in all attributes with one noticeable difference, geology. The heavily weighted geologic attribute showed noticeable differences in the landslide activity derived from the landslide inventory analysis for the Murree, Hazara and Kingriali formations which constitute 65.6% of the entire study area. These differences in secondary attribute weights show when comparing the final susceptibility maps ultimately giving the 2005 landslide susceptibility map an overall lower risk assessment. The difference in landslide activity within each formation can be attributed to the lack of training sites in the 2001 ASTER image which in turn may have impeded the feature extraction done by the Feature Analyst extension.

These results may be consulted when planning new infrastructure or mitigating a future earthquake hazard. Certain geologic formations can be circumvented when planning new construction and strategies can be prepared for accessing remote areas where highly susceptible roads and landscape may make passage impossible.

This study also shows that a continuing threat of slope failure exists immediately and at the very least six months after an earthquake event. In the six month time span between November 2005 and May 2006, freezing conditions in winter and thawing in spring had a strong impact on slope stability. The repeat photography analysis of 138 locations revealed an increase of 155 failures. Many fissures that resulted from the initial earthquake and the numerous aftershocks developed into full-fledged slope failures, often producing structural damage of infrastructure, transportation routes, and agricultural lands. The majority of the new or reactivated slope failures were found along roadways, which supports the view that human interference, particularly deforestation and the

construction and maintenance of roads, has a considerable impact on the stability of hill slopes. This study shows that there is a significant cause and effect relationship between the above mentioned anthropogenic activities and slope failure. The rebuilding effort in Northern Pakistan should take these conclusions into account during the planning and reconstruction phases after the earthquake.

Limitations of Study

There are several potential sources of error in the process of landslide susceptibility mapping. The attribute layers were gathered from various sources and several of them were digitized from a hard copy source. There is inevitably always a margin of error when geo-referencing and digitizing a geographic layer within the GIS. In this research four layers (geology, fault lines, rivers, roads, and tributaries) were digitized either using scanned hard copy maps or the 15 meter resolution ASTER satellite image. The rivers, tributaries and roads layers that were obtained from the United Nations in Islamabad were incomplete and inaccurate. Although it was possible to manually edit the rivers and tributaries, they were not easily identified on the ASTER imagery.

Another potential error that might have caused incorrectness of the final susceptibility maps is the existence of mixed pixels. This possibility of error could have occurred several times during the course of the research. The first instance was the creation of the landslide inventories; the second the land cover classification and finally the assigning of susceptibility classes to the study area. In the susceptibility classification for example the pixels (15m by 15m) often contained more than one type of susceptibility

class. This averaging of pixels values caused many pixels to be rounded, lowering the total number in the zonal statistics tool used to extract them ultimately affecting the susceptibility level assigned to them.

A bias was introduced to the study when all GPS points, used as ground truths, were taken along road and waterways due to the inaccessibility of the mountainous terrain found throughout the study area. This bias could possibly lead to lower susceptibility levels in areas which are not adjacent to roads or rivers.

The heuristic approach is an expert driven technique which is subject to the possibility of human error. The pair-wise comparison within the MCE relies on the opinions of the researcher to evaluate the importance of each attribute. The final decisions were made based mainly on observations and notes from the field and also previous studies done in the Himalaya region.

Further Research

There are three main topics to expand upon within this research. The first would be a more precise analysis of existing background landsliding activities in earthquake-prone regions. The results from such studies would help to better separate pre-earthquake and post-earthquake landsliding, which is essential for reliable landsliding prediction. The second is an analysis of the effects of the snowmelt and summer monsoon seasons on slope stability and landscape evolution. The third area of future study would be an analysis of how fast the landscape re-adjusts to its background landslide activity after an earthquake event. This type of analysis would require several more pre-earthquake

imagery scenes and would be most beneficial if worked congruently with the analysis of background landsliding rates of the region mentioned earlier.

REFERENCES

Abbasi, A., Iftikhar. Khan, M., Asif. Ishfaq, Mohammad. Mool, P., K. 2002. Slope failure and landslide mechanism, Murree area, North Paksitan. Geological Bulletin Univ. Peshawar 35, 125-137.

Abbot, Patrick, 2004. *Natural Disaster* *4th edition*. San Diego State: McGraw Hill, 208-239.

AJK Forest Department, 2001. Forestry Statistics of Azad Kashmir.

Akgun, A., Eronata. H., Turk, 2005. Comparing Different Satellite Image Classification Methods: An Application in Ayvalik District, Western Turkey. Dokuz Eylul University, Department of Geological Engineering.

Asch, W.J. 1984. Landslides: The Deduction of Strength Parameters of Materials from Equilibrium Analysis. Braunshweig 11, 39-49.

Ayalew, Luseged, Yamagishi, Hiromitsu. 1984. The application of GIS-based logistic regression for landslide susceptibility mapping in the Kakda-Yahiko Mountains, Central Japan. Geomorphology 65, 15-31.

Ayalew, Luseged., Yamagishi, Hiromitsu., Ugawa, Norimitsu. 2004. Landslide susceptibility mapping using GIS-based weighted linear combination, the case in Tsugawa area of Agano River, Niigata Prefecture, Japan. Landslides 1, 73-81.

Avouac, J.-P., Ayoub, F., Leprince, S., Konca, O., Helmberger, D.V., 2006. The 2005, M_w 7.6 Kashmir earthquake: Sub-pixel correlation of ASTER images and seismic waveforms analysis. Earth and Planetary Science Letters 249, 514–528.

Baig, M.S., 2006. Active faulting and earthquake deformation in Hazara–Kashmir Syntaxis, Azad Kashmir, northwest Himalaya. In: Kausar, A.B., Karim, T., Khan, T.(Eds.), International Conference on 8 October 2005 Earthquake in Pakistan: Its Implications & Hazard Mitigation, January 18–19, 2006, Islamabad, Extended Abstracts, pp. 27–28.

Barredo, J.I.; Benavides, A.; Hervas, J.; Van-Westen, C.J. 2000. Comparing heuristic landslide hazard assessment techniques using GIS in the Tirajana basin, Gran Canaria Island, Spain. ITC-Journal 1, 9-23.

BBC News. "Hundreds die in South Asia quake." Available from http://news.bbc.co.uk/2/hi/ south_asia/4321490.stm. Internet; accessed 24 August 2006.

Bendick, R., Bilham, R., Khan, M.A., Khan, S.F., 2007. Slip on an active wedge thrust from geodetic observations of the 8 October 2005 Kashmir earthquake. Geology 35, 267–270.

Brabb, E.E. 1984. Innovative approaches to landslide hazard mapping. *In Proceedings of 5th International Symposium on Landslides,* Rotterdam: Balkema. 1059-1074.

Brabb, E.E. 1984. Innovative approaches to landslide hazard and risk mapping. *In Proceedings 4th International Symposium on Landslides,* Toronto, Canada, Vol 1, 307-324.

Calkins, A., James, Offield W., Terry, Abdullah, S., Ali, S.K., Tayyab, S. 1975. Geology of the Southern Himalaya In Hazara, Pakistan and Adjacent Areas. Geological Survey Professional paper 716-C. United States Government Printing Office, Washington.

Carrara. A., Cardinali. R., Guzzetti,-F.; Reichenbach,-P. 1999. Use of GIS Technology in the Prediction and Monitoring of Landslide Hazard. Natural Hazards 20, 117-135.

Casagli, N., Catani, F., Puglisi, C., Delmonaco, G., Ermini, L., Margottini, C. 2004. An Inventory-Based Approach to Landslide Susceptibility Assessment and its Application to the Virginio River Basin, Italy. Environmental & Engineering Geoscience 10, 3: 203-216.

Chen, K., Blong, R., Jacobson, C. 2001. MCE-RISK: integrating multicriteria evaluation and GIS for risk decision-making in natural hazards. Environmental Modeling & Software 16, 387-397.

CIRES (Cooperative Institute for Research in Environmental Science). http://cires.colorado.edu/~bilham/Kashmir%202005.htm Accessed 28 July 2006.

Day, C. 1997. Remote sensing applications which may be addressed by neural networks using parallel processing technology. In Neuro-computation in Remote Sensing Data Analysis, edited by I. Kanellopoulos, G. G. Wilkinson, F. Roli, and J. Austin 262–279.

Earth Science Australia: Mass Wasting. http://www.earthsci.org/flood/J_Flood04/masswa/masswa.html#Gravity Accessed 12 August 2007.

Eastman, J.R., 2003. IDRISI Kilimanjaro: Guide to GIS and Image Processing' Clark Laboratories, Clark University, Worcester, USA. 123-144.

EERI "First Report on the Kashmir Earthquake of October 8, 2005" EERI Special Earthquake Report — December 2005. Available from http://www.eeri.org. Internet; accessed 15 Feburary 2006.

Fall, M., Azzam, R., Noubactep, C. 2006. A multi-method approach to study the stability of natural slopes and landslide susceptibility mapping. Engineering Geology 82, 241-263.

Foody, G.M. 2004. Supervised image classification by MLP and RBF neural networks with and without an exhaustively defined set of classes. International Journal of Remote Sensing 25, 15: 3091–3104.

Fujiwara, S., Tobita, M., Sato, H.P., Ozawa, S., Une, H., Koarai, M., Nakai, H., Fujiwara, M., Yarai, H., Nishimura, T., Hayashi, F., 2006. Satellite data gives snapshot of the 2005 Pakistan Earthquake. Eos Transactions 87, 73 and 77.

Guzzetti, F., Carrara, A., Cardinali, M. and Reichenbach, P. 1999. Landslide hazard evaluation: a review of current techniques and their application in a multi-scale study, Central Italy. Geomorphology 31, 181-216.

Harp, E.L., Crone, A.J., 2006. Landslides triggered by the October 8, 2005, Pakistan earthquake and associated landslide-dammed reservoirs. U.S. Geological Survey Open-File Report 2006-1052. 10 pp.

Huabin, Wang.; Gangjun, Liu.; Weiya, Xu.; Gonghui, Wang. 2005. GIS-based landslide hazard assessment: an overview. Progress in Physical Geography 29, 4: 548-567.

Hussain, Ahmed. 2006. Geological Survey of Pakistan, personal comm.

Hussain, A., Khan, R.N., 1996. Geological map of Azad Jammu and Kashmir. Geological Map Series. Geological Survey of Pakistan, Islamabad.

International Rivers Network: Hydrology Data and Dams. http://www.irn.org/basics/ard/index.php?id=sr-hydrology.html Accessed 10 October 2007.

Kamp, U., et al., GIS-based landslide susceptibility mapping for the 2005 Kashmir earthquake region, Geomorphology (2008), doi:10.1016/j.geomorph.2008.03.003

Kazmi, A., Jan Qasim, M. 1997. Geology and Tectonics of Pakistan. Nazimbad, Pakistan: Graphic Publishers.

Keefer, D.K., 1984. Landslides caused by earthquakes. Geological Society of America Bulletin 95, 406–421.

Keefer, D.K., 1994. The importance of earthquake-induced landslides to long-term slope erosion and slope-failure hazards in seismically active regions. Geomorphology 10,265–284.

Lan, H.X., Zhou, C.H., Wang, L.J., Zhang, H.Y., Li, R.H. 2004. Landslide hazard spatial analysis and prediction using GIS in the Xiaojiang watershed, Yunnan, China. Engineering Geology. 76, 109-128.

Landis R. J. and Koch G.G. 1977. The Measurement of Observer Agreement for Categorical Data. Biometrics. 33, 1: 159-174.

Lee, Saro., Kyungduck, Min. 2001. Statistical analysis of landslide susceptibility at Yongin, Korea. Environmental Geology. 40, 1095-1113.

Malczewski, Jacek. 1999. *GIS and Multicriteria Decision Analysis*. New York: John Wiley & Sons, Inc., 182-187.

Moreiras, S.M., 2006. Frequency of debris flows and rockfall along the Mendoza river valley (Central Andes), Argentina: associated risk and future scenario. Quaternary International 158, 110–121.

Owen, L.A., Kamp, U., Khattak, G.A., Harp, E.L., Keefer, D.K., Bauer, M.A., 2008. Landslides triggered by the October 8, 2005, Kashmir earthquake. Geomorphology 94, 1–9.

Pachauri, A.K., Gupta, P.V., Chander, R. 1998. Landslide zoning in a part of the Garhwal Himalayas. Environmental Geology 36, 3-4: 325-334.

Pararas, George. The Earthquake of 8 October 2005 in Northern Pakistan. Available from: http://www.drgeorgepc.com/Earthquake2005Pakistan.html Accessed 22 February, 2007.

Peiris, N., Rossetto, T., Burton, P., Mahmood, S. 2006. EEFIT Mission: October 8, 2005 Kashmir Earthquake. Published Report, The Institution of Structural Engineers, London, U.K., 31 pp.

Pakistan, Statistics Division. "Population Census Organization." 1998. Available from http://www.statpak.gov.pk/depts/pco /statistics/area_pop /area_pop.html. Internet; accessed 17 August 2006.

Pakistan Water Gateway, 2007. Jhelum River: Key Facts. http://waterinfo.net.pk/fsrj.htm Accessed 11 November 2007.

Pathier, E., Fielding, E.J., Wright, T.J., Walker, R., Parsons, B.E., Hensley, S., 2006. Displacement field and slip distribution of the 2005 Kashmir earthquake from SAR imagery. Geophysical Research Letters 33, L20310. doi:10.1029/2006GL027193

Roa, J. 2007. University of Maryland, personal comm.

Saaty, T. 1990. *The Analytic Hierarch Process: Planning, Priority Setting, Resource Allocation.* Pittsburgh: RWS Publications, 502 pp.

Saha, A. K., Gupta, R. P. 2002. GIS-based Landslide Hazard Zonation in the Bhagirathi (Ganga) Valley, Himalayas. International Journal of Remote Sensing, 23, 2: 357-369.

Sercombe, W.J. 1994. Wrench Faulting in the Northern Pakistan Foreland Region. The Leading Edge, 13, 11: 1107-1110.

Sudmeier-Rieux, K., Qureshi, R.A., Peduzzi, P., Nessi, J., Breguet, A., Dubois, Jaboyedoff, M., Jaubert, R., Rietbergen, S., Klaus, R., Cheema, M.A., 2007b. Disaster Risk, Livelihoods and Natural Barriers, Strengthening Decision-Making Tools for Disaster Risk Reduction, A Case Study from Northern Pakistan. The World Conservation Union (IUCN) Pakistan Program, Final Report, Karachi, 53 pp.

Thomlinson, J. R., Bolstad, P. V., & Cohen, W. B. 1999. Coordinating methodologies for scaling landcover classifications from site-specific to global: steps toward validating global map products. Remote Sensing of Environment, 70, 16– 28.

Trommler, N., Huggel, C., Korup, O., Schneider, F.J., 2008. Assessing post-failure geomorphic impact of an earthquake-triggered landslide dam, Jhelum River, Pakistan. Geophysical Research Abstracts 10 EGU2008-A-00622.

Van Westin, C. J., Rengers, N., Soeters, R. 2003. Use of Geomorphological Information in Indirect Landslide Susceptibility Assessment. Natural Hazards 30, 399-419.

Varnes, D.J., with IAEG Commission on landslides and other Mass-Movements Landslide hazard zonation: a review of principle and practices. (Paris: UNESCO Press, 1984) 63.

Varnes, D.J. 1978. Slope movement types and processes, in Schuster, R.L., and Krizek, R.J., *Landslides-Analysis and control*: National Academy of Sciences Transportation Research Board Special Report 176, 12-33.

Virdi, N.S., Sah, M.P., Bartarya, S.K., 1997. Mass wasting its manifestations, causes and control; some case histories from Himachal Himalaya. HIMAVIKAS Occasional Publication 10, 111–130.

Wang, Linlin, Ge, Hua, Xu, Caijun, Du, Zhixing, 2007. 3-D coseismic displacement field of the 2005 Kashmir earthquake inferred from satellite radar imagery. Earth Planets Space 59, 343–349.

World Meteorological Organization (WMO) "Pakistan." Available from http://www.worldweather.org /047/c00901.htm. Internet; accessed 17 August 2006.